Tectonophysics 474 (2009) 417–434

Contents lists available at ScienceDirect

Tectonophysics

journal homepage: www.elsevier.com/locate/tecto

Repeated granitoid intrusions during the Neoproterozoic along the western boundary of the Saharan metacraton, Eastern Hoggar, Tuareg shield, Algeria: An AMS and U–Pb zircon age study

B. Henry [a,*], J.P. Liégeois [b], O. Nouar [c], M.E.M. Derder [c], B. Bayou [c], O. Bruguier [d], A. Ouabadi [e], D. Belhai [e], M. Amenna [c], A. Hemmi [c], M. Ayache [c]

[a] Paléomagnétisme, IPGP and CNRS, 4 Avenue de Neptune, 94107 Saint-Maur cedex, France
[b] Isotope Geology, Royal Museum for Central Africa, B-3080 Tervuren, Belgium
[c] CRAAG, BP 63, 16340 Bouzaréah, Alger, Algeria
[d] Géosciences Montpellier, Université de Montpellier II, 34095 Montpellier, France
[e] Laboratoire "Géodynamique, Géologie de l'Ingénieur et Planétologie", FSTGAT/USTHB, BP 32, El-Alia Bab Ezzouar, 16111 Alger, Algeria

ARTICLE INFO

Article history:
Received 20 February 2009
Received in revised form 7 April 2009
Accepted 19 April 2009
Available online 24 April 2009

Keywords:
Hoggar
Pan-African
Saharan metacraton
Shear zone
Pluton
Anisotropy
Magnetic susceptibility
LA-ICP-MS U–Pb zircon dating

ABSTRACT

The N–S oriented Raghane shear zone (8°30′) delineates the western boundary of the Saharan metacraton and is, with the 4°50′ shear zone, the most important shear zone in the Tuareg shield. It can be followed on 1000 km in the basement from southern Aïr, Niger to NE Hoggar, Algeria. Large subhorizontal movements have occurred during the Pan-African orogeny and several groups of granitoids intruded during the Neoproterozoic. We report U–Pb zircon datings (laser ICP-MS) showing that three magmatic suites of granitoids emplaced close to the Raghane shear zone at c. 790 Ma, c. 590 and c. 550 Ma. A comprehensive and detailed (158 sites, more than 1000 cores) magnetic fabric study was performed on 8 plutons belonging to the three magmatic suites and distributed on 200 km along the Raghane shear zone. The main minerals in all the target plutons do not show visible preferential magmatic orientation except in narrow shear zones. The AMS study shows that all plutons have a magnetic lineation and foliation compatible with the deformed zones that are zones deformed lately in post-solidus conditions. These structures are related to the nearby mega-shear zones, the Raghane shear zone for most of them. The old c. 793 Ma Touffok granite preserved locally its original structures. The magnetic structures of the c. 593 Ma Ohergehem pluton, intruded in the Aouzegueur terrane, are related to thrust structures generated by the Raghane shear zone while it is not the case of the contemporaneous plutons in the Assodé–Issalane terrane whose structures are only related to the subvertical shear zones. Finally, the c. 550 Ma granite group has magnetic structure related to the N–S oriented Raghane shear zone and its associated NNE-SSW structures when close to them, but NW-SE oriented when further. These NW-SE oriented structures appear to be characteristic of the late Neoproterozoic evolution of the Saharan metacraton and are in relation to the convergence with the Murzuq craton. This evolution reflects the rheological contrast existing along the Raghane shear zone marking the western boundary of the Saharan metacraton.

1. Introduction

The Saharan metacraton (Abdelsalam et al., 2002), although corresponding to the eastern half of Sahara, is still largely unknown (Kilian, 1935; Lelubre, 1952; Guérangé and Vialon, 1960; Bertrand et al., 1978). Its western boundary is delimited by the Raghane shear zone (Liégeois et al., 1994), N–S oriented along the 8°30′ longitude and outcropping on 1000 km from the Aïr mountains in Niger to NE Hoggar in Algeria. To the East, the Aouzegueur, Barghot, Edembo and Djanet terranes (Black et al., 1994) belong to the Saharan metacraton but generally present its young superstructures. Their Algerian parts belong to the Eastern Hoggar, whose particularities compared to Central Hoggar have long been recognized (Bertrand and Caby, 1978). The Assodé–Issalane terrane is part of Central Hoggar, is located to the West of the Raghane shear zone and is characterized by a Pan-African high-temperature amphibolite facies metamorphism accompanied by a regional partial melting exemplified by the Renatt leucogranite and migmatites (Liégeois et al., 1994).

The main magmatic event along the Raghane shear zone occurred in the 620–580 Ma interval (Bertrand et al., 1986; Liégeois et al., 1994). Until very recently, it was considered that the Eastern Hoggar, i.e. the Hoggar part east of the Raghane shear zone, was stabilized early at

* Corresponding author. Fax: +33 1 45 11 41 90.
E-mail address: henry@ipgp.jussieu.fr (B. Henry).

0040-1951/$ – see front matter © 2009 Elsevier B.V. All rights reserved.
doi:10.1016/j.tecto.2009.04.022

c. 730 Ma, the age of an undeformed granite pluton considered as late to post-orogenic (Caby and Andreopoulos-Renaud, 1987). Current research shows that the Eastern Hoggar was actually stabilized later than the rest of Hoggar, namely at 575–545 Ma, this period including both the intrusion of granitoids and regional metamorphism (Fezaa et al., submitted for publication).

A series of batholiths and plutons intruded along the Raghane shear zone. In the field they are mostly undeformed, the deformation being localized in narrow shear zones (Liégeois et al., 1994). The main easily visible effect is the elongated shape of the intrusive bodies parallel to the Raghane shear zone but this is not the case for all plutons, some of them being roughly circular. Knowing the existence in the area of granitoids of several ages at 730 Ma, 620–580 Ma and 575–545 Ma (Bertrand et al., 1986; Caby and Andreopoulos-Renaud, 1987; Liégeois et al., 1994; Fezaa et al., submitted for publication) and even 800–820 Ma (Liégeois et al., 2005), we undertook a study of the Anisotropy of Magnetic Susceptibility (AMS — e.g. King, 1966; Hrouda et al., 1971; Henry, 1974; Djouadi and Bouchez, 1992; Archanjo et al., 1994; Borradaile and Kehlenbeck, 1996; Pignotta and Benn, 1999; Bouchez, 2000; Tomezzoli et al., 2003; Henry et al., 2004; Auréjac et al., 2004; Kratinová et al., 2007). We applied this structural method to eight undeformed plutons located along the Raghane shear zone for a better understanding of their emplacement relative to the contemporaneous tectonic stress. To reach such a goal requires dating of some representative plutons, which has been done on three of them (U–Pb laser ablation ICP-MS on zircon). The studied plutons belonging to three different stages (c. 790 Ma, c. 590 and c. 550 Ma), the study of their AMS aims at deciphering the complex interplay of the successive tectonic stresses registered by nearly strain-free plutons that occurred along a same mega shear-zone. In addition, this study provides information about the behavior of the western margin of the Saharan metacraton during the Neoproterozoic.

2. Geological setting

2.1. The Tuareg shield

The Tuareg shield (Fig. 1) is composed of 23 terranes Archaean to Neoproterozoic in age, juxtaposed after large displacements along mega-shear zones (Black et al., 1994; Liégeois et al., 1994). Most of these

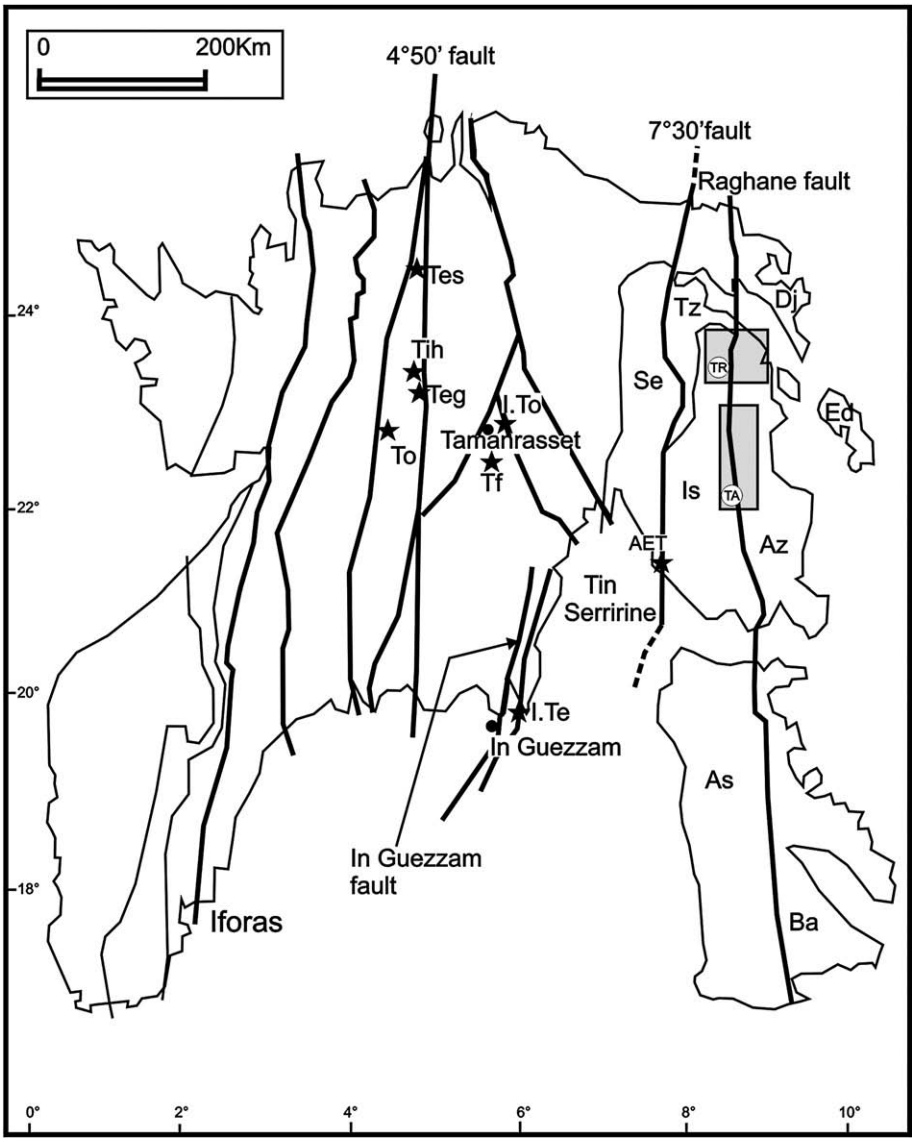

Fig. 1. General geological sketch map of the Tuareg shield showing the studied Late Panafrican plutons. Terranes of Assodé (*As*), Issalane (*Is*), Tazat (*Tz*), Aouzegueur (*Az*), Barghot (*Ba*), Djanet (*Dj*) and Edembo (*Ed*). Tihaliouine (Tih — Henry et al., 2008), Teg Orak (Teg — Henry et al., 2008), Tesnou (Tes — Djouadi and Bouchez, 1992), Alous En Tides (AET — Henry et al., 2004), In Telloukh (ITe — Henry et al., 2007), Tioueine (To — Djouadi et al., 1997), Tifferkit (Tf — Henry et al., 2006) and In Tounine (Ito — Henry et al., 2006) plutons. Tadoumet (TA) and Tiririne (TR) areas.

shear zones are N–S oriented except to the east where they are NW-SE oriented (Fig. 1). The central part of the shield (Central Hoggar) is composed of well-preserved amphibolite to granulite-facies Archaean and Paleoproterozoic terranes despite the major Pan-African reworking (Liégeois et al., 2003; Peucat et al., 2003; Bendaoud et al., 2008). They constitute the LATEA metacraton (Liégeois et al., 2003), located to the west of the Raghane shear zone (LATEA is the acronym of the terranes constituting this metacraton: Laouni–Azrou n'Fad–Tefedest–Egéré-Aleksod; Liégeois et al., 2003). The metacratonization of LATEA, marked by mega-shear zones, intrusion of batholiths (Bertrand et al., 1978; Acef et al., 2003) accompanied by high-temperature metamorphism that can reach the amphibolite facies (Bendaoud et al., 2008) occurred mainly at

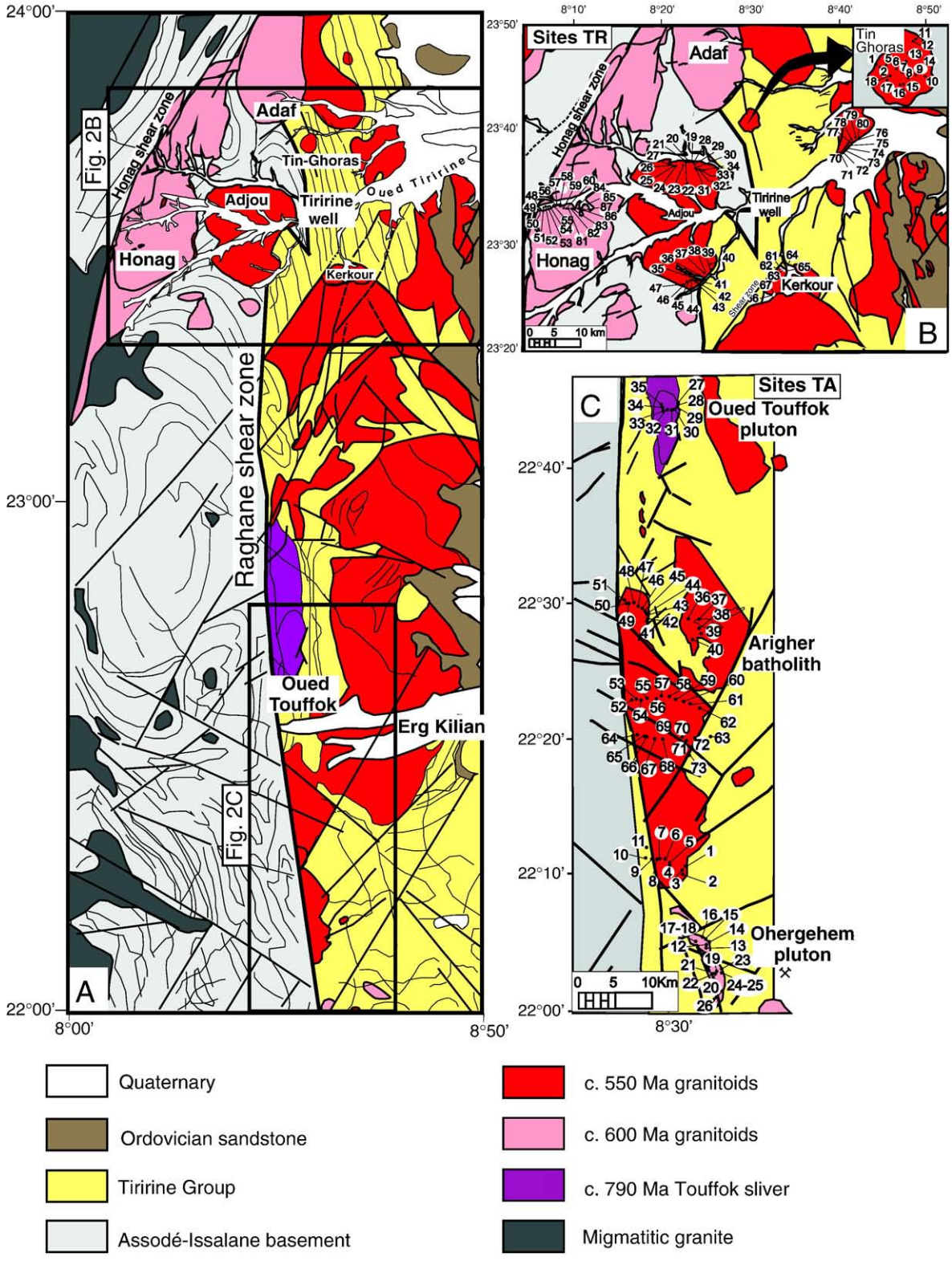

Fig. 2. Geological setting (A) — after Vialon and Guérangé (1959); Arène et al. (1961); Bertrand et al. (1978); Fomine (1990), modified — and sampling sites in the Tiririne (B — sites TR) and Tadoumet (C — sites TA) areas.

Table 1
U–Pb isotopic data on zircons (laser ICP-MS).

Sample	Pb* (ppm)	Th (ppm)	U (ppm)	Th/U	$^{208}Pb/^{206}Pb$	$^{207}Pb/^{206}Pb$	± (1σ)	$^{207}Pb/^{235}U$	± (1σ)	$^{206}Pb/^{238}U$	± (1σ)	Rho*	Apparent ages (Ma) $^{206}Pb/^{238}U$	±1σ	$^{207}Pb/^{206}Pb$	±1σ
DAZ01 — Oued Touffok (site TA27)																
la17	80	756	661	1.14	0.520	0.1172	0.0020	1.3896	0.0385	0.0860	0.0019	0.80	532	11	1915	30
la8	71	626	465	1.34	0.508	0.0857	0.0031	1.3187	0.0529	0.1116	0.0018	0.41	682	11	1332	69
sa3	91	767	628	1.22	0.319	0.0884	0.0040	1.4493	0.0689	0.1189	0.0019	0.33	724	11	1391	84
lb3	102	841	646	1.30	0.439	0.0758	0.0014	1.2587	0.0315	0.1205	0.0020	0.66	733	12	1089	37
la12	107	892	658	1.36	0.417	0.0779	0.0017	1.3087	0.0332	0.1219	0.0017	0.55	741	10	1144	42
sa4	56	398	357	1.12	0.401	0.0783	0.0023	1.3468	0.0483	0.1247	0.0025	0.56	757	14	1156	58
sa5	51	308	311	0.99	0.400	0.1075	0.0025	1.8587	0.0563	0.1254	0.0025	0.65	762	14	1757	42
la16	67	468	409	1.15	0.396	0.0658	0.0014	1.1586	0.0327	0.1276	0.0023	0.64	774	13	801	45
la2	101	699	651	1.07	0.325	0.0673	0.0011	1.1843	0.0262	0.1277	0.0020	0.70	774	11	847	32
la4	119	1020	704	1.45	0.436	0.0667	0.0012	1.1883	0.0299	0.1292	0.0022	0.68	783	13	829	38
lb2	109	843	626	1.35	0.456	0.0658	0.0015	1.1760	0.0298	0.1296	0.0015	0.46	785	9	801	47
la5	73	534	455	1.17	0.352	0.0669	0.0011	1.1976	0.0274	0.1298	0.0022	0.73	787	12	835	32
la11	74	571	464	1.23	0.353	0.0655	0.0010	1.1727	0.0230	0.1299	0.0015	0.61	787	9	789	32
la7	142	1156	847	1.36	0.414	0.0658	0.0011	1.1799	0.0231	0.1300	0.0014	0.54	788	8	801	34
la13	88	636	544	1.17	0.363	0.0657	0.0013	1.1798	0.0267	0.1302	0.0014	0.47	789	8	797	41
la24	105	821	659	1.25	0.402	0.0658	0.0014	1.1826	0.0319	0.1303	0.0021	0.60	790	12	800	45
lb5	92	754	543	1.39	0.422	0.0648	0.0006	1.1688	0.0196	0.1308	0.0018	0.81	792	10	769	21
la10	59	364	392	0.93	0.285	0.0659	0.0013	1.1913	0.0331	0.1311	0.0026	0.71	794	15	803	41
sa2	19	96	157	0.61	0.256	0.0647	0.0007	1.1722	0.0242	0.1314	0.0023	0.84	796	13	765	24
la9	67	509	434	1.17	0.342	0.0653	0.0010	1.1825	0.0237	0.1314	0.0017	0.64	796	10	783	32
la18	50	282	330	0.86	0.254	0.0662	0.0010	1.1987	0.0238	0.1314	0.0016	0.62	796	9	811	32
la23	61	397	372	1.07	0.387	0.0651	0.0055	1.1825	0.1016	0.1317	0.0018	0.16	798	10	778	169
la15	68	492	413	1.19	0.352	0.0653	0.0010	1.1866	0.0243	0.1319	0.0018	0.65	798	10	783	32
lb4	87	733	491	1.49	0.475	0.0657	0.0007	1.1973	0.0221	0.1321	0.0019	0.79	800	11	798	23
la14	95	714	556	1.28	0.403	0.0649	0.0012	1.1866	0.0267	0.1326	0.0017	0.57	803	10	771	38
la22	32	145	220	0.66	0.198	0.0668	0.0011	1.2243	0.0263	0.1329	0.0018	0.64	804	10	833	34
la3	70	403	461	0.87	0.253	0.0669	0.0011	1.2262	0.0396	0.1329	0.0037	0.86	805	21	835	34
la1	79	596	483	1.23	0.356	0.0657	0.0014	1.2065	0.0312	0.1332	0.0021	0.60	806	12	797	43
ga33	46	185	211	0.88	0.265	0.0792	0.0005	2.0461	0.0301	0.1875	0.0025	0.91	1108	14	1176	12
ga34	57	167	255	0.66	0.219	0.0844	0.0006	2.3193	0.0220	0.1993	0.0011	0.60	1171	6	1302	15
la20	94	120	436	0.27	0.096	0.0878	0.0014	2.5459	0.0474	0.2102	0.0022	0.56	1230	12	1379	29
ga37	131	222	589	0.38	0.127	0.0877	0.0007	2.6386	0.0426	0.2182	0.0030	0.86	1272	16	1376	16
la19	37	119	144	0.82	0.247	0.0835	0.0014	2.5746	0.0596	0.2236	0.0036	0.70	1301	19	1281	32
la25	95	251	367	0.68	0.207	0.0894	0.0014	2.8857	0.0579	0.2341	0.0028	0.61	1356	15	1412	30
ga35	171	735	537	1.37	0.404	0.0883	0.0005	2.9915	0.0215	0.2458	0.0012	0.66	1417	6	1388	10
la6	56	58	174	0.33	0.095	0.1126	0.0018	5.0652	0.1432	0.3263	0.0076	0.83	1821	37	1841	28
la21	76	119	509	0.23	0.087	0.0660	0.0010	1.5525	0.0498	0.1706	0.0048	0.88	1015	26	807	32
lb1	114	566	463	1.22	0.395	0.1003	0.0014	2.6634	0.0505	0.1926	0.0024	0.66	1135	13	1630	26
DAZ03 — Arigher batholith (site TA49)																
sa19	571	2811	7083	0.40	0.124	0.0581	0.0009	0.6265	0.0134	0.0782	0.0012	0.70	485	7	535	33
sa7	103	805	1134	0.71	0.259	0.0689	0.0011	0.7507	0.0182	0.0790	0.0014	0.74	490	8	896	33
la35	104	807	1194	0.68	0.205	0.0600	0.0007	0.6590	0.0138	0.0796	0.0014	0.84	494	8	604	24
la28	51	260	571	0.45	0.172	0.0678	0.0012	0.7651	0.0170	0.0819	0.0011	0.59	507	6	862	37
la33	79	353	894	0.39	0.135	0.0627	0.0012	0.7171	0.0153	0.0830	0.0007	0.42	514	4	698	41
la30	129	868	1434	0.61	0.196	0.0613	0.0010	0.7029	0.0157	0.0832	0.0013	0.69	515	8	649	34
sa17	365	1365	4296	0.32	0.106	0.0588	0.0008	0.6824	0.0135	0.0841	0.0012	0.71	521	7	561	30
sa9	116	718	1242	0.58	0.200	0.0590	0.0010	0.7117	0.0205	0.0874	0.0021	0.82	540	12	568	35
sa6	109	604	1145	0.53	0.173	0.0598	0.0007	0.7239	0.0150	0.0878	0.0015	0.84	543	9	596	24
sa12	66	302	715	0.42	0.160	0.0587	0.0008	0.7155	0.0159	0.0883	0.0015	0.77	546	9	557	31
sa16	103	637	1084	0.59	0.174	0.0585	0.0008	0.7149	0.0160	0.0886	0.0015	0.77	547	9	549	31
sa10	17	164	162	1.01	0.305	0.0586	0.0008	0.7172	0.0160	0.0887	0.0016	0.80	548	9	554	29
la34	64	557	596	0.94	0.321	0.0581	0.0025	0.7118	0.0324	0.0888	0.0013	0.32	549	8	534	92
la26	101	592	1069	0.55	0.174	0.0601	0.0011	0.7395	0.0186	0.0892	0.0015	0.68	551	9	607	40
sa14	109	617	1144	0.54	0.169	0.0583	0.0008	0.7173	0.0169	0.0892	0.0017	0.80	551	10	541	31
la32	117	1528	1065	1.43	0.406	0.0603	0.0017	0.7439	0.0271	0.0895	0.0020	0.61	552	12	614	61
la27	75	466	797	0.59	0.183	0.0616	0.0010	0.7701	0.0197	0.0906	0.0018	0.77	559	11	662	34
sa15	232	981	2490	0.39	0.133	0.0595	0.0008	0.7469	0.0171	0.0910	0.0017	0.81	561	10	587	29
la31	62	329	652	0.50	0.154	0.0585	0.0009	0.7346	0.0167	0.0910	0.0015	0.74	562	9	550	33
sa18	63	295	665	0.44	0.142	0.0581	0.0009	0.7355	0.0168	0.0919	0.0015	0.73	567	9	532	34
sa13	107	543	1099	0.49	0.148	0.0586	0.0006	0.7434	0.0146	0.0921	0.0015	0.83	568	9	550	24
la29	38	103	367	0.28	0.168	0.0859	0.0042	1.1275	0.0572	0.0952	0.0012	0.24	586	7	1337	92
sa8	82	399	780	0.51	0.199	0.0653	0.0015	0.8664	0.0226	0.0962	0.0012	0.48	592	7	786	48
DAZ04 — Ohergehem pluton (site TA16)																
sb14	24	202	213	0.95	0.286	0.0606	0.0005	0.7938	0.0119	0.0950	0.0012	0.83	585	7	624	18
sb13	18	126	172	0.73	0.223	0.0602	0.0010	0.7923	0.0173	0.0954	0.0013	0.62	587	8	612	36
sb31	20	154	177	0.87	0.267	0.0600	0.0012	0.7904	0.0193	0.0955	0.0013	0.57	588	8	605	43
sb34	19	122	161	0.76	0.220	0.0595	0.0007	0.7851	0.0137	0.0957	0.0013	0.76	589	7	586	25
sb21	15	75	153	0.49	0.152	0.0598	0.0006	0.7907	0.0125	0.0959	0.0011	0.75	590	7	597	22
sb33	30	309	269	1.15	0.283	0.0603	0.0006	0.7967	0.0135	0.0958	0.0014	0.84	590	8	614	20
sb19	22	158	193	0.82	0.263	0.0604	0.0006	0.8019	0.0129	0.0963	0.0012	0.76	593	7	618	23
sb24	24	200	245	0.82	0.245	0.0601	0.0011	0.7986	0.0224	0.0964	0.0021	0.78	593	12	607	38

Table 1 (*continued*)

Sample	Pb* (ppm)	Th (ppm)	U (ppm)	Th/U	$^{208}Pb/^{206}Pb$	$^{207}Pb/^{206}Pb$	± (1σ)	$^{207}Pb/^{235}U$	± (1σ)	$^{206}Pb/^{238}U$	± (1σ)	Rho*	Apparent ages (Ma) $^{206}Pb/^{238}U$	±1σ	$^{207}Pb/^{206}Pb$	±1σ
DAZ04 — Ohergehem pluton (site TA16)																
sb20	32	255	290	0.88	0.279	0.0605	0.0007	0.8063	0.0133	0.0966	0.0012	0.75	595	7	622	23
sb12	28	196	257	0.76	0.235	0.0607	0.0008	0.8138	0.0142	0.0972	0.0012	0.69	598	7	629	27
sb16	23	169	204	0.83	0.269	0.0601	0.0006	0.8122	0.0121	0.0981	0.0011	0.75	603	6	606	21
sb22	12	50	110	0.45	0.138	0.0607	0.0006	0.8498	0.0138	0.1015	0.0013	0.77	623	7	630	22
sb25	21	138	177	0.78	0.249	0.0625	0.0010	0.8796	0.0177	0.1021	0.0013	0.64	627	8	690	33
sb35	19	79	182	0.43	0.138	0.0608	0.0007	0.8593	0.0134	0.1024	0.0011	0.68	629	6	634	24
sb26	15	70	141	0.50	0.158	0.0642	0.0007	0.9110	0.0140	0.1030	0.0011	0.70	632	6	747	23
sb17	21	140	188	0.74	0.232	0.0623	0.0009	0.8882	0.0173	0.1033	0.0014	0.68	634	8	686	30
sb23	28	209	229	0.91	0.285	0.0618	0.0006	0.8821	0.0134	0.1036	0.0011	0.73	635	7	666	22
sb11	19	120	162	0.74	0.237	0.0658	0.0010	0.9434	0.0173	0.1040	0.0011	0.57	638	6	800	31
sb27	22	83	195	0.43	0.146	0.0653	0.0010	0.9469	0.0194	0.1052	0.0014	0.64	645	8	784	33
sb18	18	120	145	0.83	0.262	0.0613	0.0007	0.8969	0.0153	0.1061	0.0013	0.72	650	8	650	25
sb29	24	165	192	0.86	0.269	0.0625	0.0008	0.9280	0.0205	0.1077	0.0019	0.81	659	11	691	27
sb15	14	53	125	0.42	0.131	0.0639	0.0010	0.9706	0.0198	0.1101	0.0014	0.60	673	8	739	34
sb28	24	109	205	0.53	0.167	0.0617	0.0007	0.9408	0.0173	0.1106	0.0016	0.79	676	9	664	24

Pb* = radiogenic Pb; Rho* = coefficient of error correlation.

620–600 Ma (Bertrand et al., 1978; Acef et al., 2003; Bendaoud et al., 2008) and ended at c. 572 Ma, when high-level subcircular plutons such as the Temaguessine pluton intruded (Abdallah et al., 2007). Later reactivations of the same shear zones in LATEA are shown by the intrusion of subcircular alkali-calcic plutons (Boissonnas, 1974; Azzouni-Sekkal et al., 2003) up to the Cambrian (Tioueine pluton, 524 ± 1 Ma; Paquette et al., 1998).

The terranes from Eastern Hoggar, by contrast to the other Hoggar terranes, are bounded by mega-shear zones NW-SE oriented (Fig. 1), the reason why Eastern Hoggar has long been considered as distinct (Lelubre, 1952; Bertrand and Caby, 1978). These NW-SE shear zones join the major N–S oriented Raghane shear zone that marks the western boundary of the Saharan metacraton (Liégeois et al., 1994; Abdelsalam et al., 2002) to which the Eastern Hoggar terranes belong.

These terranes are the Aouzegueur, Edembo and Djanet terranes (Black et al., 1994; Fig. 1). The two most eastern terranes are not studied here. Recent data and interpretation indicate that they have been affected by a late Pan-African event: amphibolite (Edembo) and greenschist facies (Djanet) metamorphism and granitoid intrusion in the 575–545 Ma age range (Fezaa et al., submitted for publication). The Aouzegueur terrane, just east of the Raghane shear zone and studied here, comprises a c. 730 Ma old assemblage reminiscent of an oceanic context (Caby and Andreopoulos-Renaud, 1987), a detrital sedimentary sequence (the Tririne Group; Blaise, 1961; Bertrand et al., 1978) separated from the latter by an angular unconformity and intruded by a series of granitoid plutons and batholiths. Before this study, only the Arigher batholith has been dated (c. 550 Ma, Rb–Sr isochron; Zeghouane et al., 2008). The Tririne Group is more metamorphic and more deformed northward: tight folds with N–S axial plane close to the 8°30 shear zone characterize the northern half of the area while mainly moderate folding affected the southern half. Greenschist-facies conditions are locally reached to the south while they are well-developed to the north.

On the other side of the Raghane shear zone is found the Assodé–Issalane terrane. It is characterized by a high-temperature amphibolite facies metamorphism, a regional crustal leucogranite (Renatt granite) and by high-K calc-alkaline batholiths and plutons that intruded between 620 and 570 Ma (Guérangé and Lasserre, 1971; Bertrand et al., 1978; Liégeois et al., 1994; 1998).

The studied plutons are located along the Raghane shear zone, in both the Aouzegueur and Assodé–Issalane terranes (Fig. 2).

2.2. Field observation and U–Pb geochronology of the granitoids intruded along the Raghane shear zone

2.2.1. U–Pb dating analytical techniques

The zircons have been analyzed in Montpellier by laser ablation ICP-MS (Inductively Coupled Plasma Mass Spectrometer). Zircons were hand-picked in alcohol from the least magnetic concentrates (1° tilt at full amperage). Selected crystals were then embedded in epoxy resin, grounded and polished to expose internal structure. The sample mounts were used for U–Th–Pb microanalyses using a Lambda Physik COMPex 102 excimer laser generating 15 ns duration pulses of radiation at a wavelength of 193 nm. For analyses, the laser was coupled to a Element XR sector-field ICP-MS and analytical procedures followed those outlined in Bruguier et al. (2001) and given in earlier reports (e.g. Neves et al., 2006; Dhuime et al., 2007). Analyses were acquired using a 26 μm spot size of the laser beam. Unknowns were bracketed by measurements of the G91500 zircon standard (Wiedenbeck et al., 1995), which were used for mass bias and inter-element fractionation corrections. The calculated bias factors and their associated errors were then added in quadrature to the individual errors measured on each unknown. Accurate common Pb correction during laser ablation analyses is difficult to achieve, mainly because of the isobaric interference of ^{204}Hg on ^{204}Pb. The contribution of ^{204}Hg on ^{204}Pb was estimated by measuring the ^{202}Hg and assuming a $^{202}Hg/^{204}Hg$ natural isotopic composition of 0.2298. This allows monitoring of the common Pb content of the analyzed zircon domain, but corrections often resulted in spurious ages. Analyses yielding ^{204}Pb close to or above the limit of detection were thus rejected and Table 1 reports only analyses which were found to contain no common Pb.

2.3. Granitoids in the Assodé–Issalane terrane

The Assodé–Issalane terrane that extends on 800 km from north to south (Fig. 1) is characterized with a high-temperature amphibolite facies metamorphism accompanied by a regional potassic leucogranite and by numerous high-K calc-alkaline batholiths and plutons dated between 620 and 570 Ma (Guérangé and Lasserre, 1971; Bertrand et al., 1978; Liégeois et al., 1994). This metamorphic basement is a high grade assemblage of banded veined granitic to granodioritic gneisses, and a metasedimentary formation characterized by fuschsite-bearing quartzites, calc-silicate gneisses and marbles, the whole being highly deformed under ductile conditions.

This study is focused on the northern tip of the Assodé–Issalane terrane. In this area, the Adaf pluton is dated at 593 ± 17 Ma (9 zircon grains, MSWD = 0.73; recalculated from Bertrand et al., 1978 with Isoplot, Ludwig, 2003). The similar granitic *Honag pluton* is studied here and is considered as subcontemporaneous to the Adaf pluton. This pluton, just south-west of the Adaf pluton intruded along the Honag shear zone. The Honag shear zone, NNE-SSW oriented is parallel to the shear zone limiting to the west the northern tip of the Issalane–Assodé terrane, to which it is probably linked. The Honag pluton is made of a pink medium-grained calc-alkaline biotite granite.

Various enclaves, sometimes xenolithic, are locally abundant (sites TR57 and TR58): they vary from a felsic to a mafic composition and vary in size from a few cm to one hundred meters. Along the eastern boundary of the pluton, the enclaves are N–S oriented, parallel to the structures of the metamorphic country-rocks. Along its western boundary, along the NNE-SSW Honag shear zone, the granite is highly deformed, presenting a foliation strongly dipping eastward (N180°/68°E) and a lineation moderately plunging (15°) towards the south, indicating a dextral movement with a slight uplift of the western side. Further from this shear zone (close to the site TR59 — Fig. 2), discrete mylonitic bands alternate with undeformed granite. These mylonites are late, affecting indistinctly the granite, the enclaves and the late dykes. The mylonitic foliation is dipping (45°) towards the SSE.

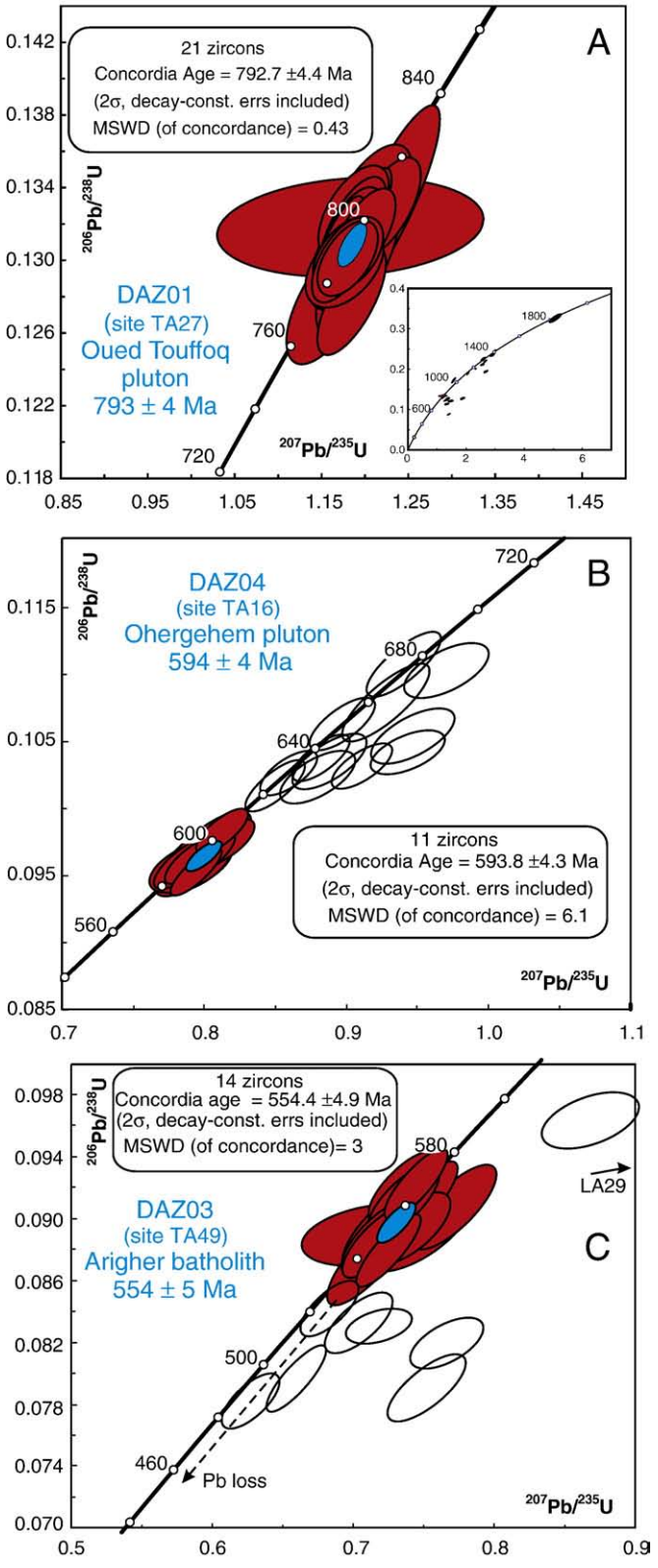

Fig. 3. U–Pb concordia diagrams for: (A) Oued Touffok pluton (sample DAZ01); (B) Tin Ohergehem pluton (sample DAZ04) and (C) Arigher batholith (sample DAZ03).

2.4. Granitoids in the Aouzegueur terrane

2.4.1. The c. 600 Ma granitoid magmatic suite

In the southern part of the studied area, the *Ohergehem* pluton is located 7 km east of the Raghane shear zone, close the Tiririne base of the ORGM. It is mainly composed of a calc-alkaline biotite-bearing granodiorite (without amphibole). Its main minerals display however a shape preferential orientation defining a foliation. The latter is present everywhere in the pluton, except on its northeastern border. Mixing–mingling features with a more mafic magma (dioritic) are observed mainly at the pluton boundaries. The same foliation is observed in both magmas. Late thin dykes of quartz diorite crosscut the main pluton and its foliation. The latter was then acquired during the magmatic crystallization of the pluton. The metamorphic country-rocks display a foliation parallel to that of the pluton.

Twenty-three zircons have been analyzed among which 11 are concordant and give a Concordia age of 594 ± 4 Ma, which is interpreted as the crystallization age of the Ohergehem pluton (Fig. 3). This age corresponds to the main movements along the Raghane shear zone and to the age of the main magmatic intrusions in the Assodé–Issalane terrane such as the Adaf pluton (Bertrand et al., 1978) and the Dabaga-west in Aïr (Liégeois et al., 1994). The twelve other zircons indicate the presence of inherited older components in this pluton. Seven analyses are concordant between 624 ± 14 Ma and 675 ± 9 Ma, the others being slightly to the right of the Concordia. Such ages are known in lithologies along the Raghane shear zone southward in the Aïr mountains in Niger (Liégeois et al., 1994).

2.4.2. The c. 550 Ma granitoid magmatic suite

The large *Arigher* batholith is N–S elongated along the Raghane shear zone around the Erg Kilian. It is considered as late to post-kinematic by Bertrand et al. (1978). The granitoids from this batholith, locally rich in dark enclaves, do not present preferential orientation of the main minerals, except close to the Raghane shear zone where they are strongly deformed and oriented. In this deformed area, the foliation is subvertical within the shear zone and steeps more to the east with a 70–80° westward plunge. Observed criteria point to a mainly dextral subhorizontal movement along the shear zone.

Twenty-three zircons have been analyzed among which 14 are concordant and give a Concordia age of 554 ± 5 Ma, which is interpreted as dating the crystallization of the Arigher batholith (Fig. 3). Five other zircons have young $^{206}Pb/^{238}U$ ages (down to 490 Ma) suggesting that they have suffered Pb loss. The four remaining zircons are located to the right of the Concordia and indicate the presence of an older component whose age cannot be specified.

The *Oued Tiririne* pluton (Fig. 2) is likely of neighboring age. It is partly covered by alluvial deposits of the dry valleys of Tafassasset and of Tiririne, but also by the discordant Tassilis Ordovician sandstones. This fine to middle-grained pink granite does not show preferential orientation of its main minerals. Only locally green enclaves display a NNE-SSW lengthening in the horizontal plane, the sole being observed. In the site TR75, a lengthening plunging of about 50° toward the NNE has been estimated.

Three other plutons, from the same magmatic suite as the Arigher batholith, have been studied.

The *Kerkour* pluton (Fig. 2) emplaced within the Tiririne series. A NE-SW-oriented fault limiting the pluton to the NW is connected to the south with the Raghane shear zone. Close this NE-SW fault, the granite is strongly deformed, with a foliation dipping 70° towards the NW and a lineation plunging 60° northward.

The *Tin Ghoras* pluton (Fig. 2) is a circular intrusion of relatively small size. The pluton forms a depression surrounded by high relief built by the sediments from the Tiririne Group transformed by contact metamorphism. The outcrops correspond to the external border of the depression and to small hills in the middle of the massif. The Tin Ghoras pluton seals a N–S fault, satellite of the Raghane shear zone. This is a pink medium-grained calc-alkaline high-K biotite granite with an equant texture. Close to the contact with the host-rocks, feldspars increase in size. Microgranitic dykes crosscut the granite. A dyke trending N120° is shifted on about 5 m by another dyke oriented N40°. Close to this second dyke, an east-dipping rough foliation striking N10° can be observed in the granite. This foliation corresponds to a well-developed plane of "en échelon" fracturation in both dykes.

The sub-circular *Adjou* pluton (Fig. 2) is located between the Honag and Tin Ghoras plutons, on the boundary between the Aouzegueur and Assodé–Issalane terranes. The Adjou granite comprises dark microgranular enclaves of mainly granodioritic composition and cm- to dm-sized. Numerous NNW-SSE dykes, mostly microgranitic in composition, crosscut the granite. These dykes generally show a N020° trending fracturation.

2.4.3. The c. 800 Ma granitoid magmatic suite

Around the Oued Touffok, an elongated area along the Raghane shear zone appears as a tectonic sliver (Fig. 2) in which intruded the *Oued Touffok* pluton, making an important relief in the landscape. This is a fine to medium-grained amphibole-biotite syenogranite. The pluton is cut in the middle by a large N–S valley, probably corresponding to a satellite fault of the Raghane shear zone. Generally undeformed, this pluton presents a visible planar shape preferential orientation of the main minerals, related to a post-magmatic deformation, in the closest site (TA31 — Fig. 2) to this valley.

Thirty-eight zircons have been analyzed among which 21 are concordant and give a Concordia age of 793 ± 4 Ma, which corresponds to the crystallization age of the Touffok pluton (Fig. 3). No concordant or subconcordant zircons give younger ages. Among the seventeen remaining analyses only strongly discordant zircon domains could indicate an effect of the main movement along the Raghane shear zone that occurred around 600 Ma. The Touffok tectonic sliver has not been

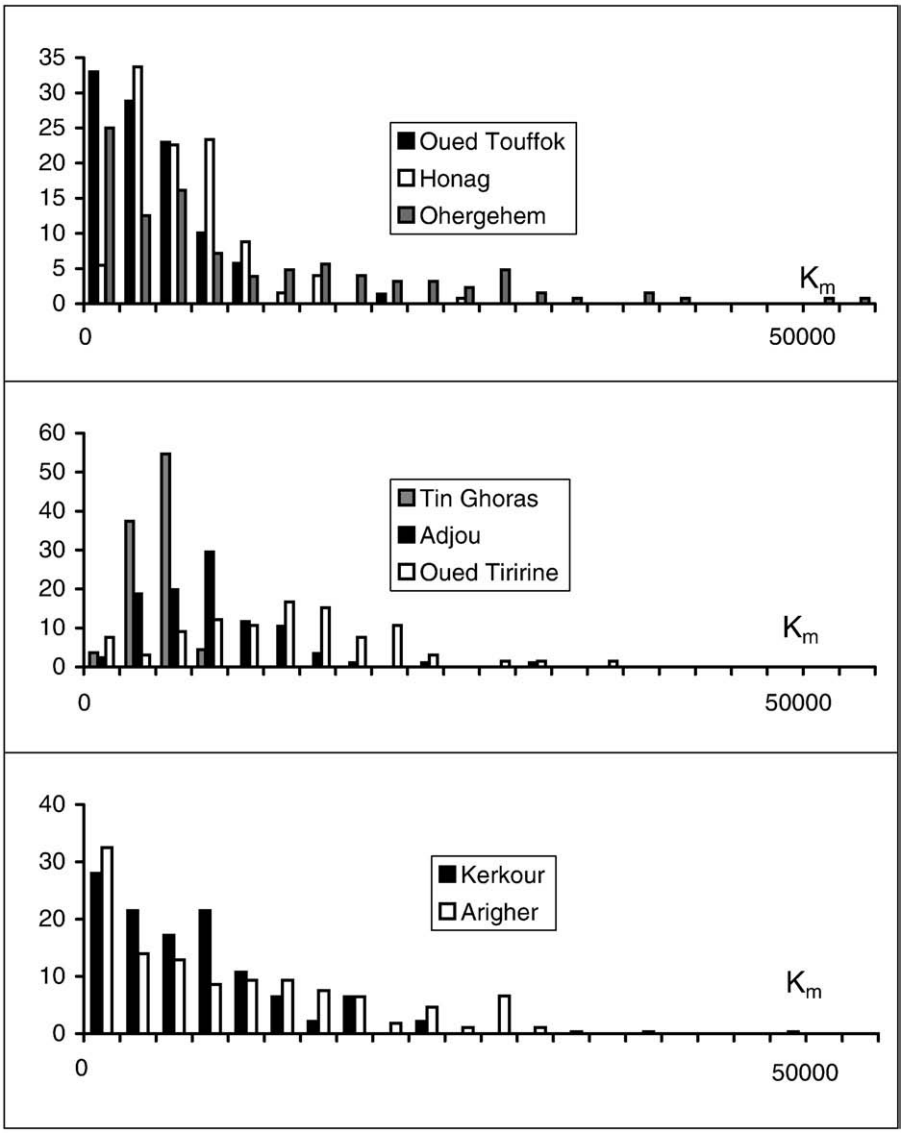

Fig. 4. Histograms in percentage of the mean susceptibility value K_m (in 10^{-6} SI) of the samples in the different studied plutons.

pervasively affected by the main Pan-African event. Another tectonic sliver along the Raghane shear zone, the Agalen area in Aïr, has also delivered zircon ages around 800 Ma with no younger ages (Liégeois et al., 2005). For Oued Touffok, nine inherited zircons spread along the Concordia from 1000 to 1400 Ma, with an additional spot at 1834 ± 46 Ma (Concordia age). This latter age is known to the west in the Gour Oumelalen area (Peucat et al., 2003) and as a whole in Hoggar, including in the Djanet sedimentary Group (Fezaa et al., submitted for publication). By opposition, Mesoproterozoic ages are lacking, as in West Africa in general (Ennih and Liégeois, 2008 and reference therein). If the subconcordant zircons with ages between 1000 and 1400 Ma have not suffered Pb loss and represent geologically meaningful ages, this would imply that the Touffok sliver is strongly exotic in Hoggar. This has to be confirmed.

3. AMS sampling sites

The 158 sampling sites (Fig. 2) have been mostly settled along cross-sections perpendicular to the main shear zones (e.g. roughly E–W). Enclaves and late-magmatic dykes were locally sampled. Where possible, the working site had a size of 50 to 200 m^2 where 6 or more cores were sampled (total sampling: 1064 cores).

- The large Arigher batholith has been sampled along 3 sections, a northern section with 16 sites (100 core-samples), a middle section with 11 sites (66 core-samples) and a southern section with 11 sites (68 core-samples). In addition, 10 sites (91 core-samples) have been chosen to the south within isolated outcrops representing apophyses of the pluton. Also, for comparison purposes, three sites have been established to the west of the Arigher batholith: two sites (TA09 and TA10) within brecciated rocks within the 8°30 shear zone and one site (TA11 with 8 core-samples) within the highly deformed rocks of the Assodé–Issalane terrane, on the other side of the Raghane shear zone.
- The small Oued Touffok pluton has been sampled in 9 sites (71 core-samples).
- The Ohergehem granite has been samples in 15 sites (120 core-samples).
- For the Honag granite, the 18 sites (125 core-samples) are located along a single section from the Honag shear zone towards the east.
- Two sampled sections are crossing the Adjou pluton, one in its northern part (16 sites, 100 core-samples) and the other in its southern part (13 sites, 85 core-samples).
- For the Tin Ghoras granite, the main E–W section (12 sites, 75 core-samples) has been completed by 6 sites (35 core-samples) along a NNE-SSW section. Two of these sites (14 core-samples) correspond to late aplitic dykes crossing the granite.
- The outcrops of the Kerkour granite are limited in size: the sampling was made along two short sections, with 5 sites (30 core-samples) in the north and 4 sites (24 core-samples) in a relatively disturbed area in the south.
- The Oued Tiririne pluton was sampled in 11 sites (66 core-samples) along a NE-SW section.

4. Rock magnetism

The mean susceptibility K_m is generally high in the studied granitoids (Fig. 4). The mean value per pluton varies between $4707 \cdot 10^{-6}$ SI for the Oued Touffok pluton and $13{,}733 \cdot 10^{-6}$ SI for the Oued Tiririne pluton. For the other plutons, this value (in 10^{-6} SI) is 9757 (Arigher), 11,403 (Ohergehem), 6864 (Honag), 8758 (Adjou), 5162 (Tin Ghoras) and 7244 (Kerkour). The values are generally homogeneous within each site, but can vary significantly from one site to another in a same intrusion. A strong weathering is clearly one of the factors affecting the mean susceptibility by decreasing its value (Henry et al., 2007): in the Oued Tiririne pluton, the strongly weathered site TR80 has K_m values varying

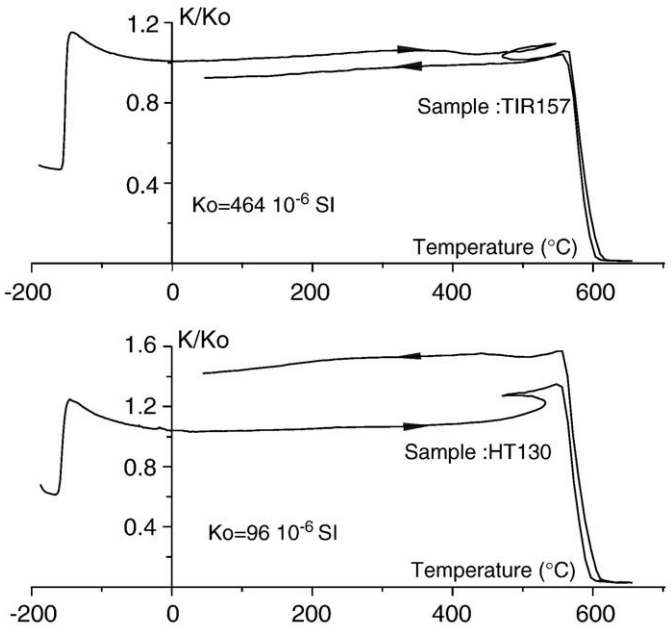

Fig. 5. Examples of normalized thermomagnetic curves of samples from the Tadoumet (sample TIR157) and Tiririne (sample HT130) areas with indication of the mean susceptibility (Ko in SI) of the sample.

from 4 to $754 \cdot 10^{-6}$ SI according to the samples while these values in the other sites of the same pluton vary from 4782 to $37{,}030 \cdot 10^{-6}$ SI. The mean susceptibility in the dykes ($70 \cdot 10^{-6}$ and $4179 \cdot 10^{-6}$ SI in the sites TR23 and TR40 of the Adjou pluton respectively, $2812 \cdot 10^{-6}$ SI in the neighboring sites TR03 and TR04 of the Tin Ghoras pluton) is lower than in their granitic host-rocks ($4218 \cdot 10^{-6}$ and $5395 \cdot 10^{-6}$ SI in the sites TR23 and TR40 respectively, $6625 \cdot 10^{-6}$ SI in the site TR02 close to the sites TR03-TR04). The enclaves of the site TR58 in the Honag pluton have higher susceptibility ($13{,}815 \cdot 10^{-6}$ SI) than the neighboring granite samples ($8345 \cdot 10^{-6}$ SI). The metamorphic rocks of the Issalane terrane in the site TA11 have very high susceptibility (0.2 SI).

Thermomagnetic analyses of low field magnetic susceptibility were carried out using a KLY-3 Kappabridge with high- and low-temperatures attachments CS2-3 (AGICO, Brno). The curves are similar for all the studied plutons, including for their aplitic dykes. For high temperatures (Fig. 5), they point out a weak mineralogical alteration during heating (Henry, 2007). They show mainly a sharp decrease of susceptibility around 580 °C, which is the Curie temperature of pure magnetite. The presence of pure magnetite is also indicated by a clear Verwey transition (Fig. 5), which corresponds to a change of mineralogical phase associated with a variation of magnetic susceptibility, occurring at low temperature. The rectangular shape of the high-temperature thermomagnetic curves and the absence of well-expressed Hopkinson peak suggest that the magnetite is of large multidomain (MD) size (O'Reilly, 1984).

Hysteresis loops were determined using a translation inductometer within an electromagnet reaching 1.6 T. The curves for all the plutons, including the aplitic dykes, are similar. Their examination (Fig. 6) reveals a weak coercive force (B_c varies from 3 to 7 mT). The values (Fig. 6) of the corresponding ratios of hysteresis parameters (Day et al., 1977) confirm that the magnetite grains of the studied granites have a large multidomain size. We can thus expect a magnetic fabric directly related to the shape of the magnetite grains.

5. Magnetic fabric

AMS in low field, measured using a KLY3 Kappabridge, yields the principal magnetic susceptibility axes maximum K_1 (magnetic lineation), intermediate K_2 and minimum K_3 (pole of the magnetic

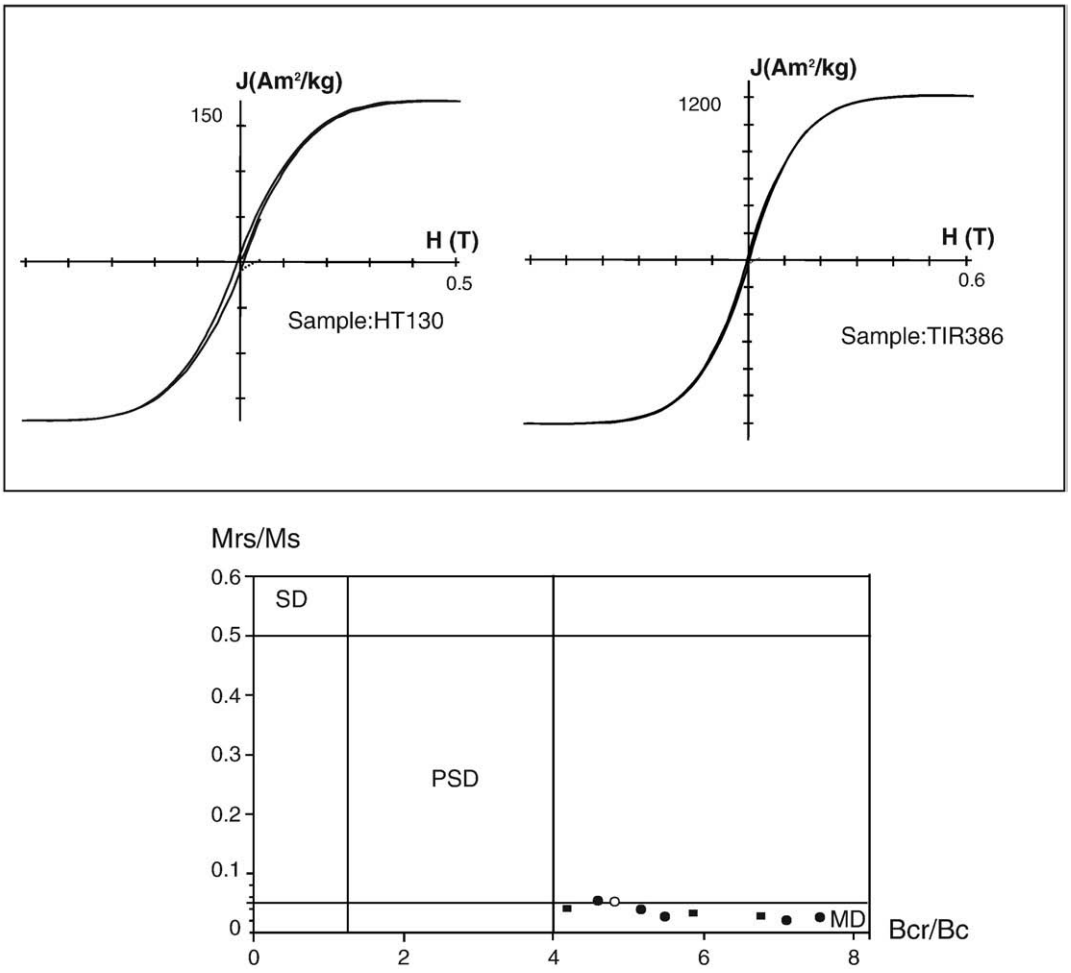

Fig. 6. Hysteresis loop after correction of the paramagnetism of samples from the Tadoumet (sample TIR386) and Tiririne (sample HT130) areas and day plot (Day et al., 1977) of the hysteresis parameters ratios of samples from Tadoumet (squares) and Tiririne (circles) areas (granite — full symbols, and aplitic dyke — open symbol); SD (single domain), PSD (pseudo-single domain) and MD (multidomain).

foliation). The Jelinek (1981) intensity P' and shape T (possibly varying from +1 for oblate to −1 for prolate) parameters were used to describe the magnetic fabric. The data for a group of samples, at the site scale as well as at the pluton scale, were analyzed using normalized tensor variability (Hext, 1963; Jelinek, 1978), simple bootstrap (Henry, 1997) and bivariate (Henry and Le Goff, 1995) statistics. For bivariate statistics (Le Goff, 1990; Le Goff et al., 1992), weighting by precision parameter k related to measurement uncertainty was applied. The three methods gave similar results. The magnetic zone axis (Henry, 1997) was determined, with its associated confidence zones at 63 and 95%, in order to obtain indications about the origin (stretching or planes intersection) of the magnetic lineation. Mean tensor data (indicated in the text by bold characters) obtained at the pluton scale generally give only a rough indication, being only clearly significant for data from pluton with coherent fabric, as in several of the studied pluton here. The comparison of P' and T values from the mean tensor and from the average of the corresponding samples data yields information about the scattering of the different principal axes in the samples.

5.1. The c. 790 Ma granitoid magmatic suite (Aouzegueur terrane)

In the Aouzegueur terrane, close to the Raghane shear zone, the old *Oued Touffok* pluton (793 ± 4 Ma), most K_1 and K_3 axes are well-clustered (Fig. 7E), but a larger scattering appears in some sites (in particular in the sites the farthest from the Raghane shear zone). The P' (from 1.023 to 1.543, mean 1.160) and T (from −0.72 to 0.76, mean 0.05) values also present some scattering. The magnetic zone axis ($D = 11°$, $I = 4°$) coincides with the mean $\boldsymbol{K}_1$ ($D = 12°$, $I = 4°$). No correlation appears between P' values and the mean susceptibility. For the mean tensor, $\boldsymbol{K}_3$ ($D = 105°$, $I = 36°$) and $\boldsymbol{K}_1$ axes are well-defined (Fig. 7F, Table 2). The $\boldsymbol{P'}$ (1.111) and $\boldsymbol{T}$ (−0.28) values are not well-specified as shown by a bootstrap application to the P'–T diagram. The more prolate shape of the mean tensor compared to the samples data reflects a scattering in the samples data larger for the magnetic foliation than for the magnetic lineation. In the single site where a post-magmatic fabric is clearly visible, magnetic and visible foliations well agree and the P' parameter presents the highest values obtained in the pluton.

5.2. The c. 600 Ma granitoid magmatic suite (Assodé–Issalane and Aouzegueur terranes)

In the Assodé–Issalane terrane, in the *Honag* pluton (593 ± 17 Ma), the principal K_1 and K_3 axes are relatively well-clustered (Fig. 7G), and the well-defined magnetic zone axis ($D = 175°$, $I = 25°$) is not significantly different from the mean $\boldsymbol{K}_1$ axis ($D = 182°$, $I = 18°$). The P' (from 1.060 to 1.414, mean 1.167) and T (from −0.77 to 0.96, mean −0.04) values again show scattering. The P' and mean susceptibility values do not present significant correlation. For the mean tensor, $\boldsymbol{K}_3$ ($D = 297°$, $I = 54°$) and $\boldsymbol{K}_1$ are well specified (Fig. 7H, Table 2). On the P'–T diagram, mean $\boldsymbol{P'}$ (1.117) and $\boldsymbol{T}$ (−0.28) values are also well-defined, as shown by bootstrapping. In the site TR49, very close to the

NNE-SSW Honag shear zone (Fig. 2), the magnetic and visible foliations and lineations coincide and the magnetic zone axis does not correspond to the $\boldsymbol{K}_1$ axis (showing that the latter is a mineral lineation). This is not the case in site TR48, located further from the shear zone and where the degree of visible deformation is lower. In the site TR59 in the "undeformed" granite close to the mylonitic zone plunging 45° toward the SSE, the magnetic foliation shows a plunge similar to that of the mylonitic zone. In addition the magnetic foliation is mostly SSE plunging, except close to the Honag shear zone. The magnetic lineation has a similar orientation in all the sites.

In the Aouzegueur terrane, the contemporaneous *Ohergehem* pluton (594 ± 4 Ma) displays most principal axes of the samples relatively well clustered, within each site as for the whole pluton, for K_1 and for K_3 axes (Fig. 7A). The mean $\boldsymbol{K}_1$ ($D = 228°$, $I = 58°$) is statistically different (non-overlapping confidence zones at 95%) from the magnetic zone axis ($D = 297°$, $I = 34°$ — Fig. 7B). The P' value varies from 1.021 to 1.556 (mean 1.250), the highest values corresponding to the highest mean susceptibilities. The T parameter value presents also a large scattering between −0.81 and 0.73 (mean 0.09). The mean tensor $\boldsymbol{K}_3$ ($D = 54°$, $I = 32°$) and $\boldsymbol{K}_1$ axes are very well-defined (Fig. 7B, Table 2). Bootstrap determination shows that the values for the mean tensor on the P'–T diagram ($\boldsymbol{P'} = 1.170$, $\boldsymbol{T} = 0.07$) are also well-defined and close to the mean sample values, confirming the weak scattering of the K_1 and K_3 axes in the samples data. In this pluton, there is a good coincidence between the magnetic foliation and the foliation determined in the field, for all the sites where it has been possible to determine it properly. On a map (Fig. 8A, B), the magnetic foliation and lineation are coherent, except on the eastern border of the pluton where the visible foliation also shows a more variable orientation.

5.3. The c. 550 Ma granitoid magmatic suite

On the boundary between Assodé–Issalane and Aouzegueur terranes, the *Adjou* pluton has been studied through two cross-

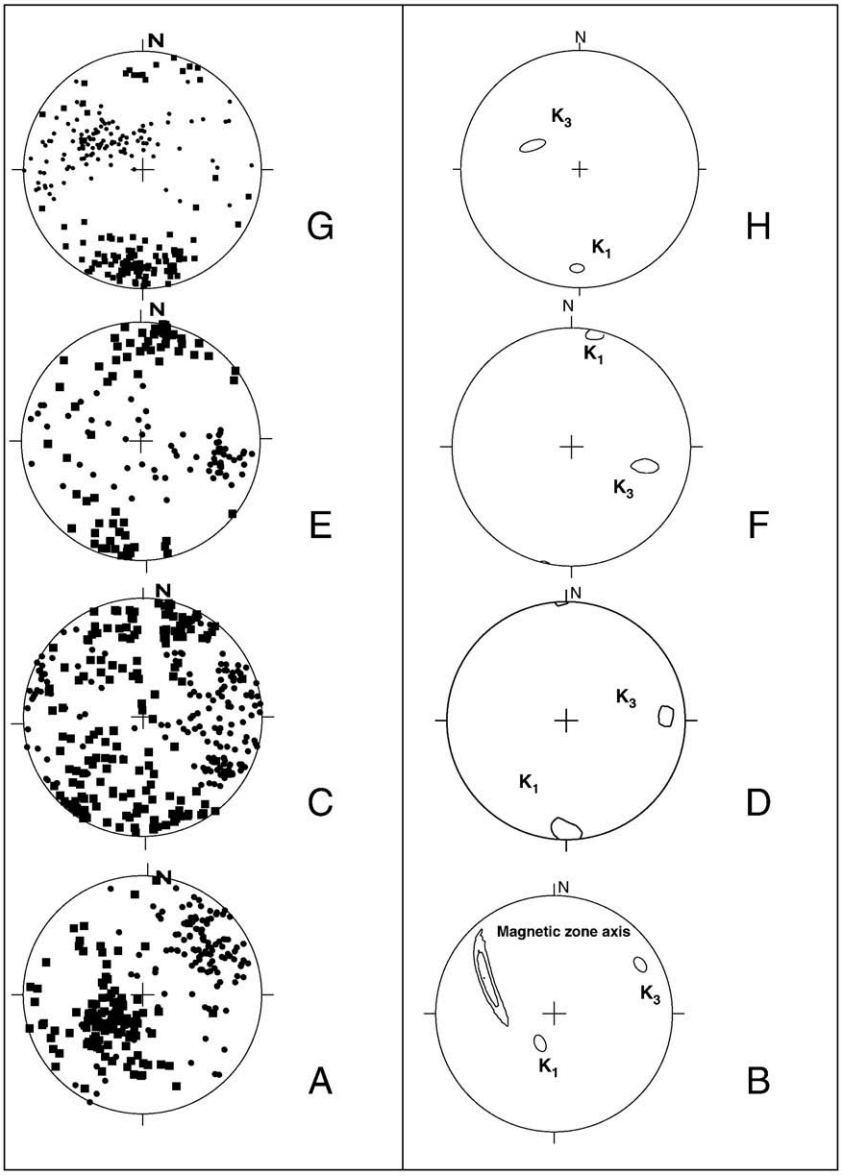

Fig. 7. Maximum (K_1, squares) and minimum (K_3, circles) principal magnetic susceptibility axes of the samples from the Ohergehem (A), Arigher (C), Oued Touffok (E), Honag (G), Adjou (I — open symbols: northern section, full symbols: southern section), Tin Ghoras (K), Kerkour (M) and Oued Tiririne (O) plutons (stereographic projection in the lower hemisphere). Confidence zone at 95% from (D, F, H, J, L, N and P) normalized tensor variability (Hext, 1963; Jelinek, 1978) or (B) simple bootstrap (Henry, 1997) statistics for the principal susceptibility axes maximum $\boldsymbol{K}_1$ (squares) and minimum $\boldsymbol{K}_3$ (circles) of the samples from the Ohergehem (B), Arigher (D), Oued Touffok (F), Honag-East (H), Adjou (J), Tin Ghoras (L), Kerkour (N) and Oued Tiririne (P) plutons (stereographic projection in the lower hemisphere); for the Ohergehem (B) pluton confidence zone at 63 and 95% for the magnetic zone axis (Henry, 1997).

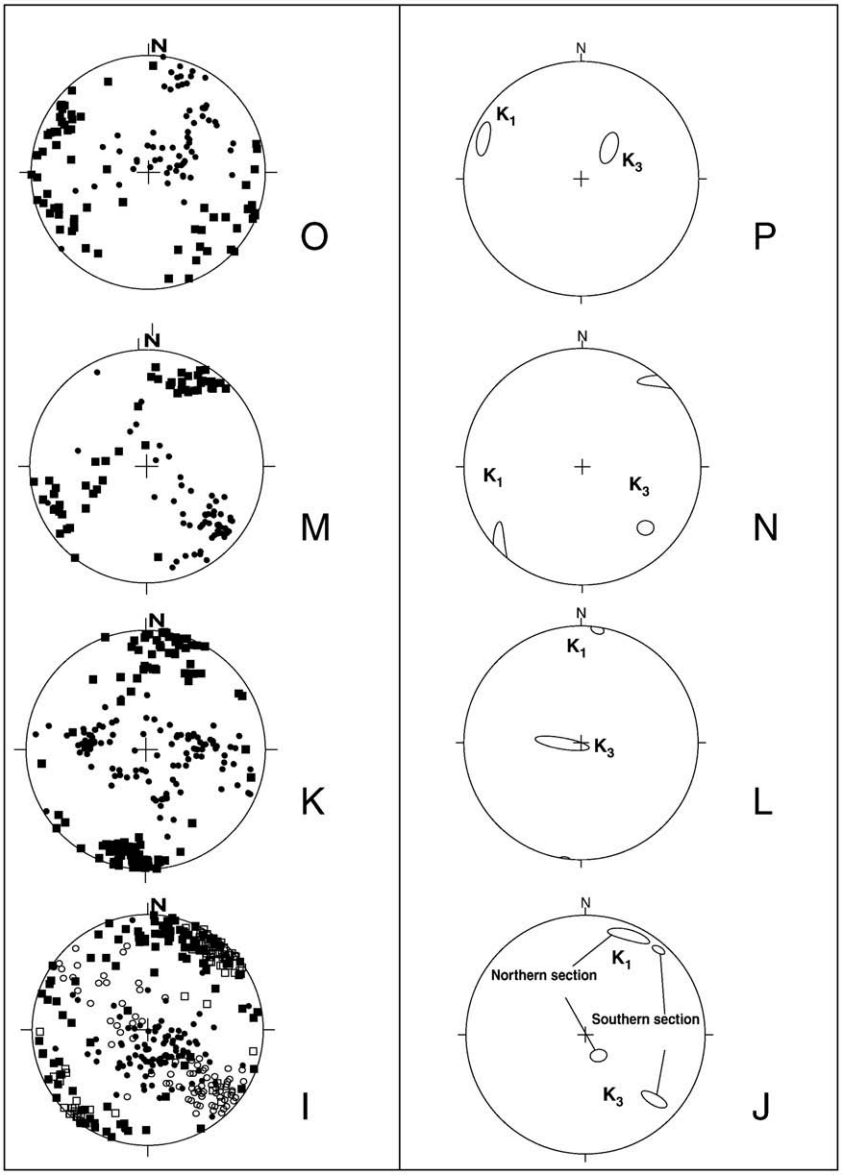

Fig. 7 (*continued*).

sections separated by 20 km (Fig. 2). Both sections (Fig. 7I) show relatively well-grouped but distinct principal axes: the obtained mean tensors (Fig. 7J, Table 2) indicate neighboring mean $\boldsymbol{K}_1$ axes ($D=25°$, $I=10°$ and $D=41°$, $I=7°$ for the northern and southern sections, respectively) but clearly different $\boldsymbol{K}_3$ axes ($D=150°$, $I=73°$ and $D=134°$, $I=22°$ for the northern and southern sections, respectively). Similarly, the mean shape is different in the northern ($\boldsymbol{T}=0.34$) and southern ($\boldsymbol{T}=-054$) sections. On a map, the orientation of the magnetic lineation is very similar for all sites from the southern section and from the middle part of the northern section.

In the *Arigher batholith* (554 ± 5 Ma) in the Aouzegueur terrane, the scattering of the principal axes of samples is relatively high with however a clear dominant orientation for K_1 as for K_3 axes (Fig. 7C). The mean $\boldsymbol{K}_1$ ($D=180°$, $I=7°$) is different from the magnetic zone axis ($D=280°$, $I=74°$). The P' values show a large variation from 1.010 to 1.736 (mean 1.148). The T parameter values present also a very large scattering between -0.94 and 0.95 (mean 0.22). For the mean tensor, well-defined mean direction for $\boldsymbol{K}_3$ ($D=88°$, $I=17°$) and for $\boldsymbol{K}_1$ can be determined (Fig. 7D, Table 2), with a lower $\boldsymbol{P}'$ value (1.067) and a more oblate shape ($\boldsymbol{T}=0.51$) when compared to the sample data. This indicates that in the sample data, the K_1 axes are more scattered than the K_3 axes. There is an excellent coincidence between the magnetic and visible foliations and lineations in all the sites located in the neighborhood of the Raghane shear zone, where a post-magmatic fabric is visible. On a map (Fig. 8C, D), the strike of the magnetic foliation is similar to that of the Raghane shear zone close to this latter. It is often rather similar to that of the NNE-SSW faults in the other parts of the pluton. The magnetic lineation also shows these both directions according to the sites.

The principal K_1 axes in the *Tin Ghoras* pluton are grouped, while K_3 axes are more scattered in the plane perpendicular to K_1, with however two main clusters (Fig. 7K). The magnetic zone axis ($D=9°$, $I=2°$) in such a case is well-defined and coincides with the mean $\boldsymbol{K}_1$ axis ($D=9°$, $I=2°$). The P' (from 1.029 to 1.185, mean 1.070) and T (from -0.87 to 0.82, mean -0.03) values show high variations and no clear correlation appears between the P' and the values of mean susceptibility. For the mean tensor, $\boldsymbol{K}_3$ ($D=268°$, $I=77°$) is associated with a lengthened confidence zone perpendicular to the well-defined $\boldsymbol{K}_1$ (Fig. 7L, Table 2). The $\boldsymbol{P}'$ (1.046) and $\boldsymbol{T}$ (-0.47) values are associated with a large confidence zone on the P'–T diagram. The shape, more prolate in the mean tensor than in the sample data, reflects the scattering of the K_3 sample data. The sites TR03 and TR04

Table 2
Site, number of core-samples (N), mean susceptibility ($\boldsymbol{K_m}$), azimuth ($\boldsymbol{Az}$) and plunge ($\boldsymbol{Pl}$) of the principal maximum ($\boldsymbol{K_1}$) and minimum ($\boldsymbol{K_3}$) – normal to the magnetic foliation – susceptibility axes, parameters $\boldsymbol{P'}$ and $\boldsymbol{T}$ (Jelinek, 1981).

Site	N	K_m (10^{-6} SI)	K_1		K_3		P'	T
			Az (°)	Pl (°)	Az (°)	Pl (°)		
Ohergehem								
TA12	8	151	257	7	0	59	1.024	−0.56
TA13	8	12,190	222	42	52	47	1.267	−0.37
TA14	10	10,938	254	30	88	60	1.090	−0.46
TA15	8	8442	190	32	64	44	1.202	0.38
TA16	8	6725	233	24	38	65	1.102	−0.39
TA17	11	4636	228	63	43	27	1.300	0.11
TA18	8	30,708	223	51	49	39	1.356	0.08
TA19	8	21,166	231	66	59	24	1.326	−0.02
TA20	8	111	259	73	53	16	1.388	0.16
TA21	8	23,168	128	67	68	22	1.341	0.13
TA22	8	5084	240	53	64	37	1.381	0.46
TA23	8	8914	180	49	31	37	1.281	−0.02
TA24	8	1531	315	34	50	7	1.053	−0.04
TA25	8	6929	239	75	56	15	1.188	−0.13
TA26	8	27,352	254	69	35	17	1.315	−0.19
Arigher								
TA01	13	8014	87	18	366	68	1.017	−0.01
TA02	7	68	360	16	265	17	1.044	−0.31
TA03	9	3444	359	26	117	34	1.259	−0.42
TA04	8	59	356	40	93	8	1.018	−0.57
TA05	9	62	197	79	3	11	1.014	0.99
TA06	8	1060	204	74	48	14	1.102	0.56
TA07	9	14,005	247	80	83	9	1.464	0.65
TA08	10	5037	357	0	267	20	1.251	0.45
TA09	10	156	237	74	78	15	1.175	0.08
TA10	8	149	292	37	54	35	1.089	−0.08
TA36	8	17,685	154	8	61	16	1.062	0.56
TA37	7	22,440	3	6	270	31	1.057	−0.55
TA38	6	5201	216	5	310	40	1.057	0.12
TA39	6	6247	38	4	128	9	1.103	0.31
TA40	6	2192	16	34	119	19	1.092	0.08
TA41	6	6410	224	38	119	19	1.148	0.50
TA42	7	9325	224	25	123	23	1.100	0.49
TA43	6	13,214	229	21	127	28	1.142	0.49
TA44	6	8028	198	31	91	27	1.046	0.70
TA45	6	17,918	217	14	108	48	1.156	0.40
TA46	6	24,218	331	16	99	66	1.129	0.47
TA47	6	25,098	372	29	32	42	1.150	0.16
TA48	6	27,532	319	44	67	18	1.176	0.15
TA49	6	52	165	6	71	31	1.274	0.87
TA50	6	11,674	167	44	64	12	1.146	0.67
TA51	6	25,335	343	17	81	24	1.398	0.83
TA52	6	4402	164	12	67	30	1.283	−0.68
TA53	6	10,647	196	1	106	4	1.115	0.37
TA54	6	7706	27	12	267	1	1.142	0.47
TA55	6	14,817	22	26	284	16	1.059	−0.11
TA56	6	12,571	167	12	125	51	1.012	0.53
TA57	6	6705	199	67	80	11	1.043	0.42
TA58	6	4038	185	21	95	2	1.061	0.16
TA59	6	2281	352	28	101	32	1.161	0.01
TA60	6	4527	25	16	117	6	1.126	−0.18
TA61	6	10,044	271	41	143	36	1.012	0.29
TA62	6	10,298	142	18	239	21	1.362	0.28
TA63	6	167	349	23	90	23	1.100	0.69
TA64	6	13,007	170	3	79	17	1.361	0.36
TA65	6	23,312	173	38	326	49	1.073	0.45
TA66	6	20,830	26	61	158	21	1.083	0.26
TA67	6	8914	181	25	72	40	1.043	0.19
TA68	7	17,376	348	2	78	21	1.075	0.06
TA69	6	7136	18	47	283	5	1.053	0.60
TA70	6	3099	1	14	92	4	1.074	−0.08
TA71	6	5408	167	22	73	10	1.209	0.09
TA72	6	10,722	136	68	40	3	1.078	0.65
TA73	7	15,335	207	9	112	26	1.093	−0.26
Issalane terrane								
TA11	8	200,063	239	44	58	47	2.800	0.60
Oued Touffok								
TA27	10	8818	23	13	152	70	1.113	0.14
TA28	8	1069	192	1	102	29	1.053	0.58
TA29	8	4943	304	10	170	76	1.056	0.39
TA30	8	4558	13	13	109	23	1.173	0.07
TA31	8	9298	191	1	101	27	1.366	−0.12
TA32	7	3158	20	11	282	34	1.210	−0.44
TA33	7	2805	346	29	97	33	1.149	0.13
TA34	8	1970	187	8	91	38	1.096	0.10
TA35	8	4775	197	24	6	36	1.100	−0.59
Honag								
TR48	6	5782	356	21	261	15	1.289	−0.32
TR49	6	4640	171	11	265	19	1.204	0.01
TR50	6	102	312	29	51	16	1.085	−0.14
TR51	6	6639	191	5	299	75	1.108	−0.63
TR52	6	9607	194	11	290	29	1.156	−0.57
TR53	6	8940	195	9	290	30	1.146	−0.26
TR54	6	10,120	182	18	309	62	1.161	−0.24
TR55	8	9010	190	18	306	54	1.154	−0.03
TR56	5	11,116	193	18	302	45	1.197	0.11
TR57	6	7061	195	30	302	28	1.136	0.01
TR58	9	10,602	183	30	299	38	1.093	−0.43
TR59	6	6780	184	23	305	50	1.104	0.10
TR60	6	11,122	173	30	337	59	1.107	0.11
TR81	6	4331	194	17	359	73	1.108	0.28
TR82	6	4715	178	22	305	56	1.151	0.10
TR83	6	5825	181	24	303	51	1.165	−0.15
TR84	6	4659	163	29	298	52	1.155	0.10
TR85	6	6440	170	20	345	70	1.124	0.10
TR86	6	3374	160	26	316	61	1.144	0.51
TR87	6	4470	171	18	344	72	1.202	0.10
Adjou								
TR19	6	11,945	51	22	198	65	1.053	−0.02
TR20	6	6814	23	9	123	47	1.063	−0.43
TR21	10	8021	214	1	116	84	1.040	0.39
TR22	6	11,831	215	2	111	80	1.037	−0.54
TR23	8	4128	244	1	336	72	1.007	0.43
TR24	6	5925	318	24	153	65	1.035	0.66
TR25	7	7192	316	19	177	65	1.045	0.60
TR26	6	9637	9	17	178	73	1.036	−0.12
TR27	6	12,369	354	11	235	68	1.035	−0.18
TR28	6	8769	23	24	174	63	1.054	0.38
TR29	7	10,657	24	14	135	56	1.045	0.30
TR30	7	7260	11	7	127	75	1.064	0.15
TR31	6	3899	199	8	86	71	1.057	0.26
TR32	6	1875	208	6	100	72	1.054	0.71
TR33	6	1229	80	7	203	78	1.038	−0.16
TR34	6	1951	30	11	148	68	1.055	0.35
TR35	6	6085	43	12	139	25	1.087	−0.24
TR36	6	9350	47	14	153	48	1.101	−0.40
TR37	6	7665	40	8	133	22	1.103	−0.64
TR38	6	9483	43	8	134	7	1.121	−0.25
TR39	6	5144	35	7	127	14	1.124	0.25
TR40	10	4179	36	17	294	35	1.099	−0.61
TR41	6	8501	220	2	129	16	1.080	−0.27
TR42	6	10,688	234	2	141	45	1.081	−0.17
TR43	6	11,537	49	10	278	75	1.043	0.10
TR44	6	13,198	48	1	241	89	1.044	−0.41
TR45	9	9251	32	7	127	37	1.065	−0.22
TR46	6	12,446	48	3	138	9	1.038	−0.53
TR47	6	9755	234	8	329	37	1.060	0.41
Tin Ghoras								
TR01	8	6462	196	4	292	57	1.055	0.11
TR02	6	6625	179	4	274	48	1.079	0.17
TR03	8	3087	5	2	272	50	1.126	0.47
TR04	6	2538	187	1	279	56	1.134	0.11
TR05	6	6845	21	0	291	58	1.051	−0.45
TR06	6	6183	202	1	72	88	1.038	−0.09
TR07	6	5254	192	9	93	48	1.057	−0.57
TR08	6	3424	192	12	82	57	1.053	0.27
TR09	6	6743	6	0	96	37	1.053	−0.33
TR10	6	5406	21	5	123	67	1.053	−0.95
TR11	6	5989	337	42	164	48	1.041	−0.16
TR12	6	3441	7	32	160	55	1.084	0.39
TR13	6	4622	33	25	229	64	1.060	0.61

Table 2 (*continued*)

Site	N	K_m (10^{-6} SI)	K_1		K_3		P′	T
			Az (°)	Pl (°)	Az (°)	Pl (°)		
Tin Ghoras								
TR14	6	5270	4	16	160	73	1.063	−0.55
TR15	6	5933	187	18	4	72	1.034	0.01
TR16	6	4441	191	17	299	46	1.032	−0.33
TR17	6	5334	184	13	76	55	1.069	−0.08
TR18	6	5495	183	10	83	43	1.063	0.35
Kerkour								
TR61	6	3196	11	19	110	25	1.108	−0.46
TR62	7	5912	25	27	134	34	1.172	0.04
TR63	6	6584	26	18	126	28	1.138	0.02
TR64	6	12,012	39	10	132	17	1.193	0.36
TR65	6	15,532	35	10	128	16	1.338	0.36
TR66	6	3931	271	61	149	16	1.169	0.33
TR67	6	3609	236	14	58	76	1.146	−0.27
TR68	6	6700	256	15	135	63	1.199	−0.53
TR69	6	7256	270	63	174	16	1.161	−0.01
Oued Tiririne								
TR70	6	14,650	246	12	68	78	1.11à	0.19
TR71	6	16,708	237	21	42	69	1.117	0.49
TR72	6	15,128	234	16	94	69	1.109	0.17
TR73	6	8659	83	2	340	80	1.082	−0.26
TR74	6	27,841	305	15	59	56	1.176	−0.05
TR75	6	9647	288	0	18	10	1.100	0.22
TR76	6	9056	143	28	255	35	1.064	−0.38
TR77	6	14,681	300	5	32	15	1.089	−0.06
TR78	6	20,498	303	15	45	38	1.212	−0.49
TR79	6	13,448	285	12	23	32	1.062	−0.21
TR80	6	754	152	15	53	29	2.302	0.57

correspond to two late-magmatic aplitic dykes of different orientations and the site TR02 to the pluton close to these dykes. The fabric is remarkably similar in orientation in these three sites (Fig. 9). The magnetic foliation corresponds to the visible foliation in the granite and to the equivalent fracture plane in the dykes. The P' values in the dykes (1.126 and 1.134 in sites TR03 and TR04 respectively) are higher than in the granite (1.079 in site TR02), although the mean susceptibility in the dykes (3087 and 2538 in 10^{-6} SI for sites TR03 and TR04 respectively) is lower than in the granite (6625 in 10^{-6} SI for site TR02). Let us notice that the fabric is more oblate in the dyke almost parallel to the magnetic foliation ($T=0.47$) than in the dyke perpendicular to this foliation ($T=0.11$); this reflects the additional flattening exerted by the dyke walls within the dykes (Henry, 1974). On a map (Fig. 8E, F), the magnetic foliation is mainly plunging to the W to NNW in the middle and eastern parts of the pluton, while it is plunging eastward in its western part.

The principal axes are relatively scattered in the *Kerkour* pluton, with however a dominant orientation for K_1 as for K_3 (Fig. 7M). The magnetic zone axis ($D=230°$, $I=12°$) is not significantly different from the mean $\boldsymbol{K}_1$ axis ($D=225°$, $I=1°$). The P' (from 1.058 to 1.421, mean 1.202) and T (from −0.73 to 0.66, mean 0.01) values present large variations. There is a rough global increase of P' values with the increase of the mean susceptibility. For the mean tensor, $\boldsymbol{K}_3$ ($D=134°$, $I=27°$) is more precisely defined than $\boldsymbol{K}_1$ (Fig. 7N, Table 2); $\boldsymbol{P}'$ (1.135) and $\boldsymbol{T}$ (0.44) values are not well defined. On a map, the axes orientation from the northern section is more coherent than those from the southern one. The magnetic lineation is plunging toward the NNE to NE in the northern section, while it is dipping toward the W to WSW in the southern one. In the sites close to the NNE-SSW border fault, the visible and magnetic fabrics show similar orientations.

The scattering of the principal axes is important in the *Oued Tiririne* pluton (Fig. 7O), as well as the variation of the P' (from 1.013 to 1.246, mean 1.120) and T (from −0.71 to 0.71, mean −0.02) values. The magnetic zone axis ($D=308°$, $I=3°$) and the mean $\boldsymbol{K}_1$ axis ($D=309°$, $I=5°$) are not significantly different. For the mean tensor, the confidence zone for $\boldsymbol{K}_3$ ($D=45°$, $I=44°$) and for $\boldsymbol{K}_1$ are both elongated (Fig. 7P, Table 2) and $\boldsymbol{P}'$ (1.127) and $\boldsymbol{T}$ (0.26) values are not precisely defined on the P'–T diagram. On a map, the magnetic foliation is plunging to the southwest in most sites. Similarly, the magnetic lineation is different in the southern (WSW-ENE) and northern (WNW-ESE) parts of the pluton. The magnetic fabric does not correspond to the fabric determined with the preferential orientation of the enclaves.

6. Discussion

6.1. Magnetic fabric-forming conditions

6.1.1. The old c. 790 Ma magmatic suite

In the old *Oued Touffok* pluton (793 ± 3 Ma), the magnetic and visible fabrics in the site TA31 are related to the post-magmatic deformation connected with movements along the Raghane shear zone. However, similar orientation of the principal axes has been obtained in most sites, but with lower $\boldsymbol{P}'$ values. This suggests that the magnetic fabric in these sites is related to the post-magmatic deformation visible in the site TA31, the decrease of the deformation intensity being outlined by the decrease of the $\boldsymbol{P}'$ values. In three sites far from the site TA31, the magnetic fabric presents a different orientation (E–W foliation). This older pluton underwent different events since its emplacement and the fabric in these three sites could be related to emplacement. This indicates that the c. 790 Ma structures are probably preserved in the Oued Touffok sliver, except close to a N–S satellite-fault of the Raghane shear zone in the middle of the pluton, pointing to a rather rigid body. This is in agreement with the tectonic structures in the Tiririne Group that skirt around the Touffok sliver (Fig. 2).

6.1.2. The main c. 600 Ma magmatic suite (Assodé–Issalane and Aouzegueur terranes)

The highly deformed area in the *Honag pluton* (593 ± 17 Ma, Assodé–Issalane terrane) corresponds to the highest $\boldsymbol{P}'$ values. Further from the shear zone, where the visible deformation is of lower intensity, the magnetic fabric becomes similar to that determined in the apparently equant granite: like in the Alous–En-Tides pluton (Henry et al., 2004), the initial magnetic fabric was not, or slightly, affected after the emplacement of the pluton. In its central part, the Honag pluton presents a narrow mylonitized zone dipping to the SSE. The magnetic foliation in the apparently undeformed granite close to this mylonitized zone is parallel to the visible foliation in the mylonitized rocks, which is not the case close to the Honag shear zone. This indicates that the shear zones present within the pluton developed at the end of the magmatic stage under the same stress. Movements along the main Honag shear zone also occurred during the emplacement of the Honag pluton, as shown by the elongated shape of the pluton along the shear zone, but they occurred also later, in a more brittle manner.

The *Ohergehem* pluton (594 ± 4 Ma) displays a strong visible fabric, demonstrated to have occurred during the crystallization of the magma, which coincides with the magnetic fabric. The latter is therefore related to the syn-magmatic deformation that already oriented the main minerals. It also coincides with the fabric of the metamorphic country-rocks. The difference between the magnetic zone axis and the $\boldsymbol{K}_1$ axis indicates that the magnetic lineation is a mineral stretching lineation and is not related to an intersection of magnetic foliations. The foliation is globally N–S while the stretching lineation is NE-SW with a plunge of 60° to the SW. This corresponds to the Dabaga-East plutons in Aïr (Liégeois et al., 1994), which have been considered as syn-thrust (Liégeois et al., 1998). These thrusts were probably associated with large movements that occurred along the Raghane shear zone. The intrusion of the Ohergehem pluton occurred during the same period as the Adaf and Honag plutons but along different structures, which can be related to the different nature of the Assodé–Issalane and Aouzegueur terrane, the latter belonging to the more rigid Saharan metacraton.

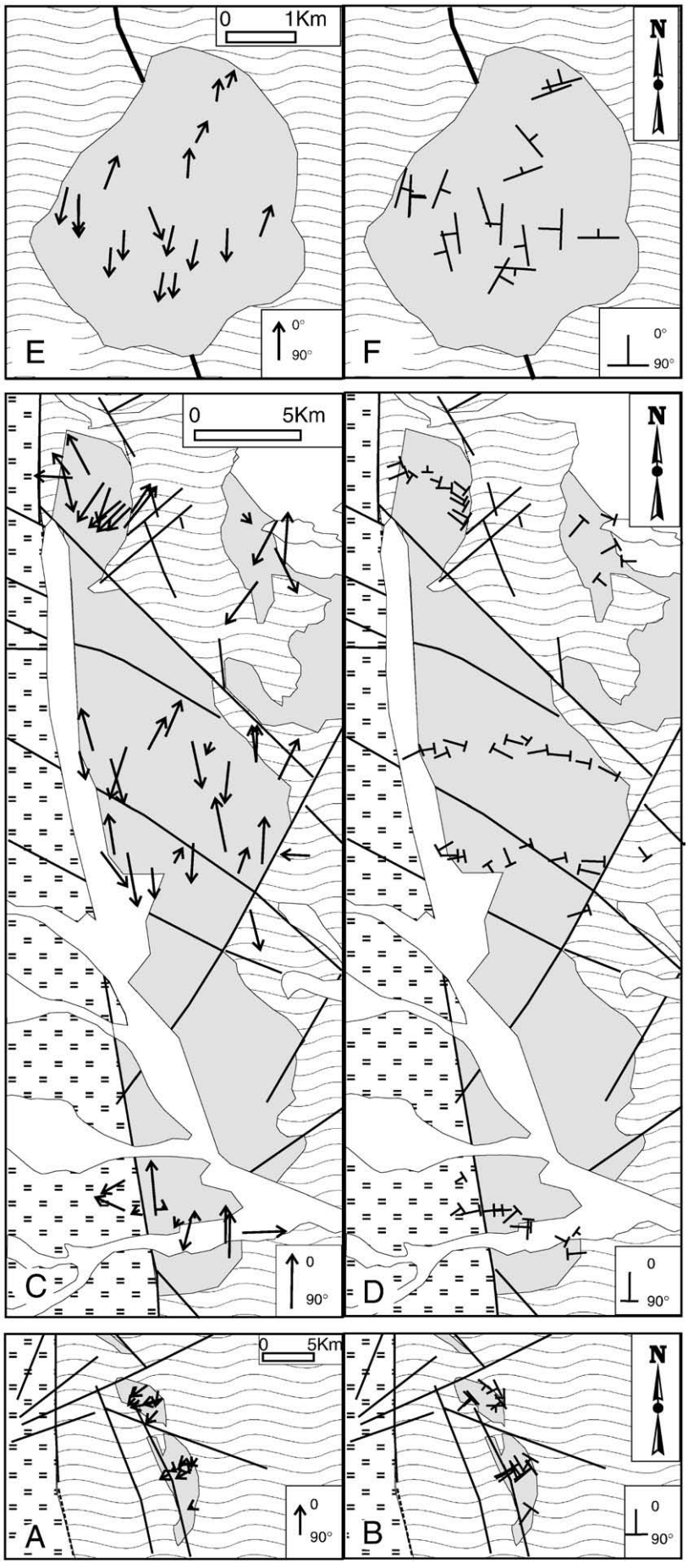
0 1Km
N
E
F
0°
90°
0 5Km
C
D
A
B
0
90°

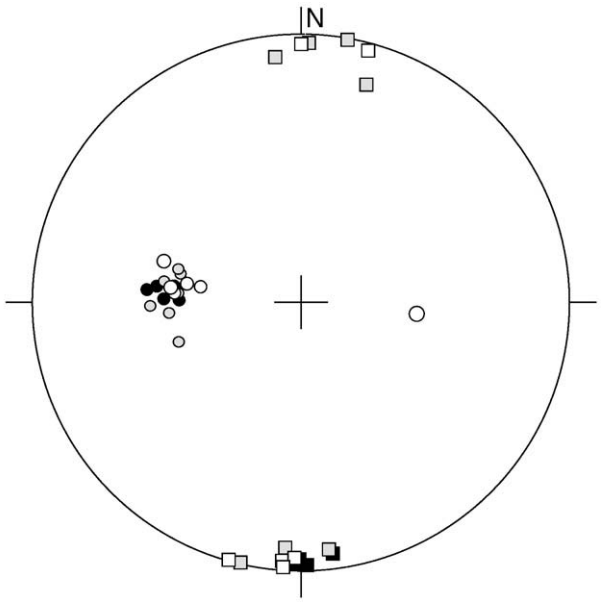

Fig. 9. Maximum (K_1, squares) and minimum (K_3, circles) principal magnetic susceptibility axes of the samples from the sites TR2 (granite — black symbols), TR3 (dyke — open gray symbols) and TR4 (dyke — open white symbols) in the Tin Ghoras pluton (stereographic projection in the lower hemisphere).

6.1.3. The c. 550 Ma magmatic event

This pluton family shares similar characteristics. They are all intrusive within the Tiririne greenschist facies sedimentary Group, pointing to a common relatively shallow depth of intrusion. Except close to shear zones, the main minerals do not show a significant shape preferential orientation. The stress contemporaneous to the crystallization was thus weak and not able to induce deformation or flow orientation within the crystallizing mush. However, the magnetic fabric is well developed (high P' values) and homogeneous within each pluton. The magnetic zone axis did not allow interpreting the origin of the magnetic lineation, except in the Arigher batholith: for the latter, the difference between the magnetic zone axis and the $\boldsymbol{K}_1$ axis indicates that the latter is related to a mineral stretching lineation.

When the "frame" of the granite is acquired by the crystallization of the main minerals, the stress environment changed from the "hydrostatic" to the "anisotropic" type. The anisotropy of the magnetite, which crystallized mostly during this period, reflects the regional stress conditions during the late-magmatic stage. This is confirmed by the homogeneity of the magnetic fabric in all these plutons, particularly the magnetic lineation orientation that is independent from the plutons shape. This is not always the case for the magnetic foliation, which sometimes shows, for example in Tin Ghoras pluton, coherent variations in the orientation. Such variations are probably partly related to the shape of the intrusion, as it was already observed in the eastern part of the Teg Orak pluton (Henry et al., 2008). An interesting example for the fabric-forming conditions is given by the Oued Tiririne pluton. This granite often includes lengthened dark microgranular enclaves whose preferential orientation indicates the flow direction during the initial magma emplacement. This direction is not reflected by a shape preferential orientation of the main minerals, which therefore crystallized mainly after the initial flowing. Measured magnetic fabric is also independent from the flow direction, though relatively coherent in the whole pluton. The magnetic fabric therefore corresponds to the late-magmatic crystallization stage when the magma was not moving a lot anymore. These fabric-forming conditions during the late-magmatic stages are also indicated by the similar fabric observed in the granite and in the late aplitic dykes in the Tin Ghoras pluton.

The *Arigher* pluton is affected by a strong deformation on its western border along the Raghane shear zone. Like in the Honag granite, the magnetic foliation is parallel to the shear zone and P' values are high (higher than 1.2). Further east, the magnetic foliation becomes striking NNE-SSW and P' values are lower (between 1.04 and 1.17). The NNE-SSW direction is that of several important fractures crossing the pluton and could be conjugated with the Raghane shear zone.

The *Kerkour* granite is strongly deformed along its northwestern border that follows a NNE-SSW fault. The magnetic fabric presents a similar orientation in the deformed and in the equant areas of the pluton. The P' values in the different sites cannot be reliably compared due to the important variation of the mean susceptibility. The shape of the susceptibility ellipsoid changes progressively towards the east in the northern section from rather prolate ($\boldsymbol{T}=-046$) very close to the fault, to neutral ($\boldsymbol{T}=0.03$) and rather oblate ($\boldsymbol{T}=0.36$) in the east, without any significant change in the orientation of the sub-horizontal NNE-SSW magnetic lineation. This indicates a syn-tectonic emplacement of the Kerkour with the tectonic movements lasting longer than the crystallization, leading to post-magmatic structures along the fault and only high-temperature orientation (AMS) in the rest of the pluton. This tectonic activity corresponds to a strain-slip movement along the fault.

The *Tin Ghoras* and *Adjou* plutons have a well-clustered sub-horizontal magnetic lineation and more variable orientation of the magnetic foliation. The magnetic lineations have a direction NNE-SSW to N–S close to that of the main shear zones (8°30 and Honag) and reflects a shearing background related to these shear zones that should have functioned contemporaneously. Both plutons do not show deformed areas. They intruded within N–S structures (Raghane shear zone and one of its satellite-fault) which seem to have not been active after the pluton emplacement.

The *Oued Tiririne* pluton is the only pluton studied here that is located far eastward from the Raghane shear zone. The magnetic lineation is sub-horizontal like in the other studied plutons, but with a very different direction (WNW-ESE). The magnetic foliation is mainly SW-dipping with variable plunge. This orientation is parallel to the shear zones separating the Aouzegueur, Edembo and Djanet terranes that are considered as generated during the 575–545 Ma time interval due to the late interaction with the Murzuq craton (Fezaa et al., submitted for publication).

6.2. Tectonic movements and granitoid emplacement along the Raghane shear zone, western boundary of the Saharan metacraton

The main movements along the Raghane shear zone occurred at around 600 Ma, the main Pan-African event in the Tuareg shield (Bertrand et al., 1978; Black et al., 1994; Liégeois et al., 1994; 2003). This movement is a N–S movement through transpression along the western boundary of the Saharan metacraton, inducing a dextral subhorizontal movement and by secondary thrusts towards the east (Liégeois et al., 1994), i.e. towards the Saharan metacraton, here represented by the Aouzegueur terrane.

The Ohergehem pluton (594 ± 4 Ma) displays a structure in agreement with that model: it is close to the Raghane shear zone with AMS lineations and foliation indicating that it intruded within the thrust structures associated with the Raghane shear zone within the Aouzegueur terrane.

The Honag pluton (593 ± 17 Ma, age of the very similar and neighbor Adaf pluton) intruded in a peculiar area, at the northern tip of the Assodé–Issalane terrane, where it is closing in a spoon-shape structure. This means that this pluton was affected by both the shear zones delimiting this terrane to the east (the Raghane shear zone) and

Fig. 8. Maps of the Ohergehem (A, B), Arigher (C, D) and the Tin Ghoras (E, F) plutons with the distribution of magnetic lineations (A, C, E) and magnetic foliations (B, D, F) measured in the studied sites. The length of the symbols (arrow for lineations, plunge indication for foliation) is proportional to the plunge values (scale on the figure).

to the west (the Honag shear zone being a major satellite fault of the main shear zone located slightly to the west). The AMS N–S lineation and NNE-SSW foliation indicate that these plutons intruded during movements along these main shear zones that therefore functioned contemporaneously. The discrete deformed parts seen in the fields, present along the pluton boundaries and as discrete elongated sheared areas within the pluton, have the same direction as the magnetic lineations: this indicates that the movements along the shear zones continued some time after the crystallization of the magmas in more brittle conditions.

The c. 600 Ma was thus the period of the northward movement of the Assodé–Issalane terrane along the western boundary of the Saharan metacraton, only affected by secondary thrust structures along the Raghane shear zone. These movements have been probably facilitated by the magma intrusions. The cessation of these movements probably occurred soon after the cessation of the magmatic intrusions of this magmatic suite, i.e. not long after 590 Ma. This is in agreement with the age of the late Temaguessine pluton more to the west (582 ± 5 Ma, SHRIMP U–Pb zircon age; Abdallah et al., 2007), considered as closing the main Pan-African phase in LATEA (Central Hoggar; Abdallah et al., 2007).

During that large movement of the Assodé–Issalane terrane, some tectonic slivers were transported along the Raghane shear zone, whose origins remain enigmatic. This is the case of the Touffok sliver that behaved as a small rigid body during the main Pan-African event: the subcircular Touffok granite present in this sliver has been dated here at 793 ± 4 Ma, preserved locally its magmatic ASM structures; its central part has been affected by a satellite-fault of the Raghane shear zone. Currently, this age range is not known in Hoggar and this sliver could be exotic. A link would be possible with the c. 730 Ma age known in to the SE in the Aouzegueur terrane (Caby and Andreopoulos-Renaud, 1987) but this has to be assessed and falls beyond the aims of this paper.

The Tiririne formation is only weakly deformed and metamorphized in the southern studied area while the degree of both deformation and metamorphism strongly increases northwards. Bertrand et al. (1978) even pointed that this formation was overlain by a limited thrusting by Assodé–Issalane series. This implies a weak clockwise rotation of a large block of the Assodé–Issalane border relatively to Aouzegueur terrane. This is a consequence of the rheological contrast between Assodé–Issalane and Aouzegueur terranes.

In the Oued Tiririne pluton, located further from the Raghane shear zone, the lineations are NW-SE oriented, parallel to the main shear zones bounding the Aouzegueur terrane to the east, separating it from the Edembo terrane. This orientation is the same as the shear zone separating the Edembo and the Djanet terrane whose functioning has been established at 570–545 Ma (Fezaa et al., submitted for publication) and due to convergence with the Murzuq terrane. We can then relate the intrusion of this pluton to this event: the NW-SE shear zones separating the Djanet, Edembo and Aouzegueur terranes merged with the Raghane shear zone that they reactivated on its northern section, reactivation that deformed and metamorphosed the Tiririne Group. This event appears thus to be mainly restricted to the Saharan metacraton. With such an assumption, this pluton should be slightly older than the last plutons that intruded within the already deformed Tiririne formation.

The last granitoid magmatic suite occurred at c. 550 Ma, as marked by the large Arigher batholith dated at 554 ± 5 Ma (U–Pb zircon, this study) and at 553 ± 20 Ma (Rb–Sr isochron, Zeghouane, 2006; Zeghouane et al., 2008). The Arigher batholith has N–S magnetic foliation and subhorizontal lineation when close to the Raghane shear zone but a NNE-SSW orientation can be observed eastwards. A neighboring, but more coherent, pattern appears also in the northern plutons which show a regular evolution of the mean magnetic fabric from the NW to the SE: The relatively close Tin Ghoras and the northern section of Adjou give the same magnetic fabric, with subhorizontal lineation slightly deviated toward the NNE-SSW while in the southern section of Adjou this deviation is stronger; a NNE-SSW orientation, parallel to NNE-SSW shear zone, is reached in the Kerkour pluton. In the same locations, mean magnetic foliation evolves from subhorizontal (Tin Ghoras and northern Adjou section) to strong NW-plunge (Southern Adjou and Kerkour). Moreover, the last displacements along the shear zones, N–S to the south and NNE-SSW to the north, likely corresponded again to a very weak clockwise rotation of a large block on the Assodé–Issalane border relatively to the Aouzegueur terrane. All this evolution clearly illustrates the major role of the N–S Raghane shear zone and of its associated NNE-SSW shear zones in the final structuration of all the western Aouzegueur border, as the consequence of the Murzuq event.

The western limit of the Saharan metacraton, marked by the Raghane shear zone remained a major separation between terranes of very contrasted rheology during the whole Pan-African and late Pan-African period. It acted as a western boundary for the c. 550 Ma Murzuq-related event and as a major boundary during the c. 600 Ma main Pan-African event.

7. Conclusion

The N–S oriented Raghane mega-shear zone marks the western boundary of the Saharan metacraton and is one of the major tectonic boundaries in the Hoggar, main part of the Tuareg shield. It separates the Aouzegueur terrane to the east, affected at most by a greenschist facies metamorphism and belonging to the Saharan metacraton, from the Assodé–Issalane terrane, affected by a Pan-African high-temperature amphibolite facies metamorphism to the west (Liégeois et al., 1994).

We have dated here by the U–Pb laser ICP-MS on zircon method three magmatic suites of granitoids that appear in the field as mostly undeformed. These are:

(1) the Touffok granite (793 ± 4 Ma) present in an old tectonic sliver;
(2) the Ohergehem pluton (594 ± 4 Ma) from the south of the Aouzegueur terrane close to the Raghane shear zone, an age that corresponds to the main granitic event in the Assodé–Issalane terrane (Bertrand et al., 1978; Liégeois et al., 1994);
(3) the Arigher batholith (554 ± 5 Ma) from the Aouzegueur terrane; this magmatic suite is not known in the Assodé–Issalane terrane but is known more to the east in the Djanet and Edembo terranes. This magmatic suite is typical of the Saharan metacraton.

The AMS (Anisotropy of Magnetic Susceptibility) that we conducted on 8 plutons among which are the three dated bodies allow us to conclude that:

(1) The pluton parts that appear undeformed in the field have a magnetic lineation and foliation compatible with the deformed zones seen in these plutons close to the shear zones. This means that these plutons are syn-tectonic and that the deformed parts seen in the field are zones deformed in post-solidus conditions, the shear stress continuing when the magma has crystallized.
(2) The magnetic structure of all plutons is related to the nearby mega-shear zones, the Raghane shear zone for most of them, i.e. a N–S to NNE-SSW subhorizontal stretching lineation and a subvertical foliation generated by the northward movement of the Assodé–Issalane terrane along the western boundary of the Saharan metacraton marked by the Raghane shear zone.

Other structures of major importance are however seen:

(1) In the old Touffok tectonic sliver, the c. 793 Ma Touffok granite has a structure related to the Raghane shear zone in its central part but preserved locally its emplacement structure.
(2) In the c. 600 Ma granite magmatic suite, a NE-SW lineation in the western part of the plutons studied in the Assodé–Issalane terrane (Honag pluton), reflecting the influence of the shear zone

marking the western boundary of this terrane; this pluton is indeed located at the northern tip of the terrane where the two boundaries, eastern and western, are converging; in the Ohergehem pluton, the foliation is globally N–S while the stretching lineation is NE-SW with a plunge of 60° to the SW, which correspond to the thrust structures associated with the Raghane shear zone on its eastern side as in Aïr (Liégeois et al., 1994).

(3) The c. 550 Ma granite magmatic suite has a structure related to the Raghane shear zone or its associated NNE-SSW structures when close to them, whatever the size of the body, whatever the Arigher batholith or the small Tin Ghoras pluton is concerned. When further from the Raghane shear zone, which is the case of the Oued Tiririne pluton, the lineation is NW-SE oriented, parallel to the main shear zones bounding the Aouzegueur terrane to the east, and characteristic of the Saharan metacraton in the Tuareg shield, resulting from a convergence with the Murzuq craton (Fezaa et al., submitted for publication). The northern part of the Raghane shear zone was reactivated by these late NW-SE oriented shear zones in which they merged. This event appears thus to be mainly restricted to the Saharan metacraton.

Acknowledgements

This project is supported by the DEF-CNRS cooperation program between Algeria and France. We are very grateful to the civil and military authorities at Tamanrasset and Djanet, to the "Office du Parc National de l'Ahaggar" (OPNA) and to the "Office du Parc National du Tassili" (OPNT) for their help. Positive comments by G. Borradaile and M.S. Petronis improved significantly the quality of the paper.

References

Abdallah, N., Liégeois, J.P., De Waele, B., Fezaa, N., Ouabadi, A., 2007. The Temaguessine Fe-cordierite orbicular granite (Central Hoggar, Algeria): U–Pb SHRIMP age, petrology, origin and geodynamical consequences for the late Pan-African magmatism of the Tuareg shield. J. Afr. Earth Sci. 49, 153–178.

Abdelsalam, G., Liégeois, J.-P., Stern, R.J., 2002. The Saharan metacraton. J. Afr. Earth Sci. 34, 119–136.

Acef, K., Liégeois, J.P., Ouabadi, A., Latouche, L., 2003. The Anfeg post-collisional Pan-African high-K calc-alkaline batholith (Central Hoggar, Algeria), result of the LATEA microcontinent metacratonization. J. Afr. Earth Sci. 37, 295–311.

Archanjo, C.J., Bouchez, J.L., Corsini, M., Vauchez, A., 1994. The granite pluton of Pombal: magnetic fabric and place within the Brasiliano strike-slip tectonics of NE-Brazil. J. Struct. Geol. 16, 323–335.

Arène, J., Blaise, J., Bourgeois, M., Bouvet, M., Byramjee, R., Guérangé, B., Illy, P., Reboul, C., Roche, J., Vialon, P., Lelubre, M., 1961. Geological map "Tazrouk". Bureau de Recherches Minières de l'Algérie and Bureau de Recherches Géologiques et Minières.

Auréjac, J.B., Gleizes, G., Diot, H., Bouchez, J.L., 2004. Le complexe granitique de Quérigut (Pyrénées, France) réexaminé par la technique de l'ASM: un pluton syntectonique de la transpression dextre hercynienne. Bull. Soc. Géol. Fr. 175, 157–174.

Azzouni-Sekkal, A., Liégeois, J.-P., Bechiri-Benmerzoug, F., Belaidi-Zinet, S., Bonin, B., 2003. The "Taourirt" magmatic province, a marker of the closing stage of the Pan-African orogeny in the Tuareg shield: review of available data and Sr–Nd isotope evidence. J. Afr. Earth Sci. 37, 331–350.

Bendaoud, A., Ouzegane, K., Godard, G., Liégeois, J.P., Kienast, J.R., Bruguier, O., Drareni, A., 2008. Geochronology and metamorphic *P–T–X* evolution of the Eburnean granulite-facies metapelites of Tidjenouine (Central Hoggar, Algeria): witness of the LATEA metacratonic evolution. In: Ennih, N., Liegeois, J.P. (Eds.), The Boundaries of the West African Craton. Geol. Soc., London, Spec. Pub., vol. 297, pp. 111–146.

Bertrand, J.M.L., Caby, R., 1978. Geodynamic evolution of the Pan-African orogenic belt: a new interpretation of the Hoggar shield. Geol. Rundsch. 67, 357–388.

Bertrand, J.M.L., Caby, R., Ducrot, J., Lancelot, J., Moussine-Pouchkine, A., Saadallah, A., 1978. The late Pan-African intracontinental fold belt of the Eastern Hoggar (central Sahara, Algeria): geology, structural development, U/Pb geochronology, tectonic implications for the Hoggar shield. Precambrian Res. 7, 349–376.

Bertrand, J.M.L., Michard, A., Boullier, A.M., Dautel, D., 1986. Structure and U/Pb geochronology of Central Hoggar (Algeria): a reappraisal of its Pan-African evolution. Tectonics 5 (955.972).

Black, R., Latouche, L., Liégeois, J.-P., Caby, R., Bertrand, J.M., 1994. Pan-African displaced terranes in the Tuareg shield (Central Sahara). Geology 22, 641–644.

Blaise, J., 1961. Sur la stratigraphie des séries anté-cambriennes dans la région du Tafassasset moyen (Ahaggar oriental). Bull. Soc. Géol. Fr. III, 184.

Boissonnas, J., 1974. Les granites à structures concentriques et quelques autres granites tardifs de la chaîne pan-africaine en Ahaggar (Sahara central, Algérie). Thèse, Centre de Recherches sur les Zones Arides, Série Géologie 16, 662 pp.

Borradaile, G.J., Kehlenbeck, M.M., 1996. Possible cryptic tectono-magnetic fabrics in "post-tectonic" granitoid plutons of the Canadian shield. Earth Planet. Sci. Lett. 137, 119–127.

Bouchez, J.L., 2000. Anisotropie de susceptibilité et fabrique des granites. Compt. Rend. Acad. Sci., Paris, Earth Planet. Sci., 330: 1–14.

Bruguier, O., Telouk, P., Cocherie, A., Fouillac, A.M., Albarede, F., 2001. Evaluation of Pb–Pb and U–Pb laser ablation ICP-MS zircon dating using matrix-matched calibration samples with a frequency quadrupled (266 nm) Nd-YAG laser. Geostand. Newsl. 25, 361–373.

Caby, R., Andreopoulos-Renaud, U., 1987. Le Hoggar oriental, bloc cratonisé à 730 Ma dans la chaîne pan-africaine du nord du continent africain. Precambrian Res. 36, 335–344.

Day, R., Fuller, M., Schmidt, V.A., 1977. Hysteresis properties of titanomagnetites: grain size and compositional dependence. Phys. Earth Planet. Inter. 13, 260–267.

Dhuime, B., Bosch, B., Bruguier, O., Caby, R., Pourtales, S., 2007. Age, provenance and post-deposition metamorphic overprint of detrital zircons from the prograde metasedimentary sequence of the Nathorst Land group (Eleonore Bay Supergroup, NE Greenland) — a LA-ICP-MS and SIMS study. Precambrian Res. 155, 24–46.

Djouadi, M.T., Bouchez, J.L., 1992. Structure étrange du granite du Tesnou (Hoggar, Algérie). C. R. Acad. Sci. Paris 315 II, 1231–1238.

Djouadi, M.T., Gleizes, G., Ferré, E., Bouchez, J.L., Caby, R., Lesquer, A., 1997. Oblique magmatic structures of two epizonal granite plutons, Hoggar, Algeria: late orogenic emplacement in a transcurrent orogen. Tectonophysics 279, 351–374.

Ennih, N., Liégeois, J.P., 2008. The boundaries of the West African craton, with a special reference to the basement of the Moroccan metacratonic Anti-Atlas belt. In: Ennih, N., Liégeois, J.P. (Eds.), The Boundaries of the West African Craton. Geol. Soc., London, Spec. Pub., vol. 297, p. 117.

Fezaa, N., Liégeois, J.-P., Abdallah, N., Cherfouh, E.H., De Waele, B., Bruguier, O., Ouabadi, A. submitted for publication. The Djanet terrane (Eastern Hoggar, Algeria), the Pan-African metacratonic boundary of the Murzuq craton: field, detrital and magmatic U–Pb zircon and Sr–Nd isotopes evidences. Precamb. Res.

Fomine, A., 1990. Field map of Tadoumet, Office national de la Recherche Géologique et Minière (ORGM).

Guérangé, B., Vialon, P., 1960. Le Pharusien du bassin de Djanet dans la région du Tafassasset moyen (Ahaggar oriental, Sahara central). C. R. Somm. Séances Soc. Géol. Fr. 3, 557–559.

Guérangé, B., Lasserre, M., 1971. Etude géochrnologique de roches du Hoggar oriental par la méthode du strontium. C. R. Somm. Séances Soc. Géol. Fr. 4, 213–215.

Henry, B., 1974. Sur l'anisotropie de susceptibilité magnétique du granite récent de Novate (Italie du Nord). C. R. Acad. Sci. Paris 278C, 1171–1174.

Henry, B., 1997. The magnetic zone axis: a new element of magnetic fabric for the interpretation of the magnetic lineation. Tectonophysics 271, 325–329.

Henry, B., 2007. Changes in magnetic mineralogy due to heating and methodological implications. Encyclopedia of Geomagnetism and Paleomagnetism, Springer Edit, pp. 512–515.

Henry, B., Le Goff, M., 1995. Application de l'extension bivariate de la statistique de Fisher aux données d'anisotropie de susceptibilité magnétique: intégration des incertitudes de mesure sur l'orientation des directions principales. C. R. Acad. Sci. Paris 320 II, 1037–1042.

Henry, B., Djellit, H., Bayou, B., Derder, M.E.M., Ouabadi, A., Merahi, M.K., Baziz, K., Khaldi, A., Hemmi, A., 2004. Emplacement and fabric-forming conditions of the Alous-En-Tides granite, eastern border of the Tin Serririne/Tin Mersoï basin (Algeria): magnetic and visible fabrics analysis. J. Struct. Geol. 26, 1647–1657.

Henry, B., Derder, M.E.M., Bayou, B., Ouabadi, A., Belhai, D., Hemmi, A., 2006. Magnetic fabric of Late Panafrican plutons in the Tamanrasset area (Hoggar shield, Algeria) and structural implications. Afr. Geosci. Rev. 13, 41–52.

Henry, B., Bayou, B., Derder, M.E.M., Djellit, H., Ouabadi, A., Khaldi, A., Hemmi, A., 2007. Late Panafrican evolution of the main Hoggar fault zones: implications of magnetic fabric study in the In Telloukh pluton (Tin Serririne basin, Algeria). J. Afr. Earth Sci. 49, 211–221. doi:10.1016/j.jafrearsci.2007.09.004.

Henry, B., Derder, M.E.M., Bayou, B., Guemache, M.A., Nouar, O., Ouabadi, A., Djellit, H., Amenna, M., Hemmi, A., 2008. Inhomogeneous shearing related with rocks composition: evidence from a major late-Panafrican shear zone in the Tuareg shield (Algeria). Swiss J. Geol. 101, 453–464. doi:10.1007/s00015-008-1262-4.

Hext, G., 1963. The estimation of second-order tensors, with related tests and designs. Biometrika 50, 353.

Hrouda, F., Chlupáčová, M., Rejl, L., 1971. The mimetic fabric in some foliated granodiorites as indicated by magnetic anisotropy. Earth Planet. Sci. Lett. 11, 381–384.

Jelinek, V., 1978. Statistical processing of magnetic susceptibility measured in groups of specimens. Stud. Geophys. Geod. 22, 50–62.

Jelinek, V., 1981. Characterization of the magnetic fabric of rocks. Tectonophysics 79, 63–67.

Kilian, C., 1935. Explorations sahariennes. Geogr. J. 86, 17–25.

King, R.F., 1966. The magnetic fabric of some Irish granites. Geol. J. 5, 43–66.

Kratinová, Z., Schulmann, K., Edel, J.B., Ježek, J., Schaltegger, U., 2007. Model of successive granite sheet emplacement in transtensional setting: integrated microstructural and anisotropy of magnetic susceptibility study. Tectonics 26, TC6003. doi:10.1029/2006TC002035.

Le Goff, M., 1990. Lissage et limites d'incertitudes des courbes de migration polaire: pondération, des données et extension bivariate de la statistique Fischer. C. R. Acad. Sci. Paris 311 II, 431–437.

Le Goff, M., Henry, B., Daly, L., 1992. Practical method for drawing a VGP path. Phys. Earth Planet. Inter. 70, 201–204.

Lelubre, M., 1952. Recherches sur la géologie de l'Ahaggar central et occidental (Sahara central). Bull. Serv. Carte Géol. Algérie, 22, tome 1, 354 p., tome 2, 387p.

Liégeois, J.P., Black, R., Navez, J., Latouche, L., 1994. Early and late Pan-African orogenies in the Aïr assembly of terranes (Tuareg shield, Niger). Precambrian Res. 67, 59–66.

Liégeois, J.P., Navez, J., Hertogen, J., Black, R., 1998. Contrasting origin of post-collisional high-K calc-alkaline and shoshonitic versus alkaline and peralkaline granitoids. Lithos 45, 1–28.

Liégeois, J.P., Latouche, L., Boughrara, M., Navez, J., Guiraud, M., 2003. The LATEA metacraton (Central Hoggar, Tuareg shield, Algeria): behaviour of an old passive margin during the Panafrican orogeny. J. Afr. Earth Sci. 37, 161–190.

Liégeois, J.P., Benhallou, A., Azzouni-Sekkal, A., Yahiaoui, R., Bonin, B., 2005. The Hoggar swell and volcanism: reactivation of the Precambrian Tuareg shield during Alpine convergence and West African Cenozoic volcanism. In: Foulger, G.R., Natland, J.H., Presnall, D.C., Anderson, D.L. (Eds.), Plates, Plumes and Paradigms. Geol. Soc. America Spec, Paper, vol. 388, pp. 379–400.

Ludwig, K.R., 2003. User's manual for Isoplot/ 3, a geochronological toolkit for Microsoft Excel. Berkeley Geochronology Center, Spec. Pub., vol. 14. 71 pp.

Neves, S., Bruguier, O., Vauchez, A., Bosch, D., Rangel da Silva, J.M., Mariano, G., 2006. Timing of crust formation, deposition of supracrustal sequences, and Transamazonian and Brasiliano metamorphism in the East Pernambuco belt (central domain, Borborema Province, NE Brazil): implications for western Gondwana assembly. Precambrian Res. 149, 197–216.

O'Reilly, W., 1984. Rock and Mineral Magnetism. Blackie, Chapman and Hall edit, Glasgow.

Paquette, J.L., Caby, R., Djouadi, M.T., Bouchez, J.L., 1998. U–Pb dating of the end of Pan-African orogeny in the Tuareg shield: the post-collisional syn-shear Tioueine pluton (Western Hoggar, Algeria). Lithos 45, 245–253.

Peucat, J.J., Drareni, A., Latouche, L., Deloule, E., Vidal, P., 2003. U–Pb zircon (TIMS and SIMS) and Sm–Nd whole rock geochronology of the Gour Oumalelen granulitic basement, Hoggar massif, Tuareg shield, Algeria. J. Afr. Earth Sci. 37, 229–239.

Pignotta, G.S., Benn, K., 1999. Magnetic fabric of the Barrington Passage pluton, Meguma Terrane, Nova Scotia: a two-stage fabric history of syntectonic emplacement. Tectonophysics 307, 75–92.

Tomezzoli, R.N., McDonald, W.D., Tickyj, H., 2003. Composite magnetic fabrics and S–C structure in granitic gneiss of Cerro de los Viejos, La Pampa province, Argentina. J. Struct. Geol. 25, 159–169.

Vialon, P., Guérangé, B., 1959. Geological maps “Erg Kilian” and “Tiririne” — “Mission hélicoptère 1958–59”. Bureau de Recherches Minières de l'Algérie.

Wiedenbeck, M., Allé, P., Corfu, F., Griffin, W.L., Meier, M., 1995. Three natural zircon standards for U–Th–Pb, Lu–Hf, trace element and REE analyses. Geostand. Newsl. 19, 1–23.

Zeghouane, H. 2006. Pétrologie, géochimie, géochimie isotopique et géochronologie Rb/Sr du massif granitique d'Arirer (terrane Aouzegueur, Hoggar oriental) Algérie. Th. Magister Univ. Sc. Technologie Houari Boumédiène, Alger.

Zeghouane, H., Azzouni-Sekkal, A., Liégeois, J.P., 2008. Pétrologie et géochronologie des granitoïdes du massif d'Arirer, (Aouzegueur, Hoggar oriental, Algérie). Abstract, 22th Colloquium of African Geology, Tunis, Tunisia, p. 259.